

AD-A066 390

NAVAL POSTGRADUATE SCHOOL MONTEREY CALIF

F/G 4/2

A STUDY OF INTERANNUAL AND INTRAANNUAL TROPICAL ATMOSPHERIC CIR--ETC(U)

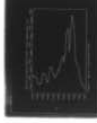
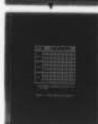
DEC 78 E L MCCORMICK

UNCLASSIFIED

NL

OF  
ADA  
066390

1



END  
DATE  
FILMED

5-79

DDC

LEVEL #

2  
NW

AD A0 66390

# NAVAL POSTGRADUATE SCHOOL

Monterey, California



DDC FILE COPY

DDC  
RECEIVED  
MAR 27 1979  
A

## THESIS

A STUDY OF INTERANNUAL AND INTRAANNUAL  
TROPICAL ATMOSPHERIC CIRCULATIONS  
DURING NORTHERN HEMISPHERE SUMMER

by

Earle Leslie McCormick

December 1978

Co-Advisor:  
Co-Advisor:

C. P. Chang  
K. M. W. Lau

Approved for public release; distribution unlimited.

79 03 26 045

REPORT DOCUMENTATION PAGE		READ INSTRUCTIONS BEFORE COMPLETING FORM
1. REPORT NUMBER	2. GOVT ACCESSION NO.	3. RECIPIENT'S CATALOG NUMBER
4. TITLE (and Subtitle) A Study of Interannual and Intraannual Tropical Atmospheric Circulations During Northern Hemisphere Summer,		5. TYPE OF REPORT & PERIOD COVERED Master's Thesis, December 1978
7. AUTHOR(s) Earle Leslie/McCormick		6. PERFORMING ORG. REPORT NUMBER
9. PERFORMING ORGANIZATION NAME AND ADDRESS Naval Postgraduate School Monterey, California 93940		8. CONTRACT OR GRANT NUMBER(s)
11. CONTROLLING OFFICE NAME AND ADDRESS Naval Postgraduate School Monterey, California 93940		10. PROGRAM ELEMENT, PROJECT, TASK AREA & WORK UNIT NUMBERS
14. MONITORING AGENCY NAME & ADDRESS (if different from Controlling Office) <i>12 57p.</i>		12. REPORT DATE December 1978
		13. NUMBER OF PAGES 56
		15. SECURITY CLASS. (of this report) Unclassified
		15a. DECLASSIFICATION/DOWNGRADING SCHEDULE
16. DISTRIBUTION STATEMENT (of this Report) Approved for public release; distribution unlimited.		
17. DISTRIBUTION STATEMENT (of the abstract entered in Block 20, if different from Report)		
18. SUPPLEMENTARY NOTES		
19. KEY WORDS (Continue on reverse side if necessary and identify by block number)		
20. ABSTRACT (Continue on reverse side if necessary and identify by block number) This thesis contains a study of the interannual and intra-annual tropical atmospheric circulations for the Northern Hemisphere summer seasons of 1974, 1975 and 1976 using satellite observations of infrared radiation and albedo in conjunction with parameters available from conventional 200 mb data. The 200 mb flow regimes are contrasted for the three seasons and power spectra and cross-spectral analysis are used to find		

DD FORM 1473  
1 JAN 73

EDITION OF 1 NOV 68 IS OBSOLETE  
S/N 0102-014-6601

SECURITY CLASSIFICATION OF THIS PAGE (When Data Entered)

251 450

1

79 03 26.04 LB

Cont

significant correlations between the parameters from time series generated within a given area and between the areas. These areas were picked for each parameter to represent regions of maximum time-averaged values. The anomalously warm sea surface temperatures in 1976 (Beprestis, 1977) occurred in conjunction with major circulation changes paralleling Bjerknes' (1969) hypothesis and the differences in flow regimes between a normal and dry monsoon season are in general agreement with Kanamitsu and Krishnamurti (1978). Significant correlations were found to exist between parameters within the eastern Pacific and western Pacific and also between these two regions. Particularly strong correlations involved the  $u^2$ ,  $v^2$  and IR parameters.

sq u      sq v

ACCESSION FOR	
RTIS	White Section <input checked="" type="checkbox"/>
ODC	Grey Section <input type="checkbox"/>
UNCLASSIFIED	<input type="checkbox"/>
JUSTIFICATION	
BY	
DISTRIBUTION/AVAILABILITY CODES	
DIRT	AVAIL. CODE OR SPECIAL
A	

Approved for public release; distribution unlimited.

A Study of Interannual and Intraannual  
Tropical Atmospheric Circulations  
During Northern Hemisphere Summer

by

Earle Leslie McCormick  
Captain, United States Air Force  
B.S., Saint Louis University, 1973

Submitted in partial fulfillment of the  
requirements for the degree of

MASTER OF SCIENCE IN METEOROLOGY

from the  
NAVAL POSTGRADUATE SCHOOL  
December 1978

Author Earle Leslie McCormick

Approved by: Harold Lee (for C-P Cheng)  
Thesis Co-Advisor

Harold Lee  
Thesis Co-Advisor

George J. Haltiner  
Chairman, Department of Meteorology

William M. Tolles  
Dean of Science and Engineering

## ABSTRACT

This thesis contains a study of the interannual and intra-annual tropical atmospheric circulations for the Northern Hemisphere summer seasons of 1974, 1975 and 1976 using satellite observations of infrared radiation and albedo in conjunction with parameters available from conventional 200 mb data. The 200 mb flow regimes are contrasted for the three seasons and power spectra and cross-spectral analysis are used to find significant correlations between the parameters from time series generated within a given area and between the areas. These areas were picked for each parameter to represent regions of maximum time-averaged values. The anomalously warm sea surface temperatures in 1976 (Bepristis, 1977) occurred in conjunction with major circulation changes paralleling Bjerknes' (1969) hypothesis and the differences in flow regimes between a normal and dry monsoon season are in general agreement with Kanamitsu and Krishnamurti (1978). Significant correlations were found to exist between parameters within the eastern Pacific and western Pacific and also between these two regions. Particularly strong correlations involved the  $u^2$ ,  $v^2$  and IR parameters.

TABLE OF CONTENTS

I. INTRODUCTION - - - - - 10

II. DATA AND ANALYSIS TECHNIQUE - - - - - 13

    A. DATA SOURCES - - - - - 13

        1. Satellite Data - - - - - 13

        2. Upper Air Data - - - - - 13

    B. DATA PERIOD - - - - - 13

    C. PARAMETERS CALCULATED - - - - - 14

        1. U-component - - - - - 14

        2. V-component - - - - - 14

        3. Divergence - - - - - 14

        4. Relative Vorticity - - - - - 15

        5. Stream Function - - - - - 15

        6. Velocity Potential - - - - - 16

    D. AREAS OF INTEREST - - - - - 16

    E. TIME SERIES PRODUCED - - - - - 17

    F. STATISTICAL ROUTINE - - - - - 17

III. RESULTS - - - - - 18

    A. COMPARISON OF THE THREE YEARS - - - - - 18

        1. Mean Circulations - - - - - 18

        2. Divergence - - - - - 20

        3. Relative Vorticity - - - - - 21

        4. Velocity Potential - - - - - 21

        5. Nondivergent Circulations - - - - - 22

B.	POWER SPECTRA	- - - - -	22
C.	COHERENCE SQUARES	- - - - -	24
	1. Monsoon System Relationships	- - - - -	25
	2. Mid to Eastern Pacific System Relationships	- - - - -	29
	3. Inter-system Relationships	- - - - -	29
IV.	CONCLUSIONS	- - - - -	31
	LIST OF REFERENCES	- - - - -	55
	INITIAL DISTRIBUTION LIST	- - - - -	56

LIST OF TABLES

I.	Power Spectra 1974-76	- - - - -	23
II.	Monsoon System Coherence Squares 1974-76	- - - - -	26
III.	Mid to Eastern Pacific System Coherence Squares 1974-76	- - - - -	27
IV.	Monsoon System-Mid to Eastern Pacific System Coherence Squares 1975-76	- - - - -	28

## LIST OF FIGURES

1.	200 mb seasonal mean U-component 1974	- - - - - 32
2.	200 mb seasonal mean U-component 1975	- - - - - 33
3.	200 mb seasonal mean U-component 1976	- - - - - 34
4.	200 mb seasonal mean V-component 1974	- - - - - 35
5.	200 mb seasonal mean V-component 1975	- - - - - 36
6.	200 mb seasonal mean V-component 1976	- - - - - 37
7.	200 mb seasonal mean divergence 1974	- - - - - 38
8.	200 mb seasonal mean divergence 1975	- - - - - 39
9.	200 mb seasonal mean divergence 1976	- - - - - 40
10.	200 mb seasonal mean relative vorticity 1974	- - - 41
11.	200 mb seasonal mean relative vorticity 1975	- - - 42
12.	200 mb seasonal mean relative vorticity 1976	- - - 43
13.	200 mb seasonal mean velocity potential 1974	- - - 44
14.	200 mb seasonal mean velocity potential 1975	- - - 45
15.	200 mb seasonal mean velocity potential 1976	- - - 46
16.	200 mb seasonal mean stream function 1974	- - - 47
17.	200 mb seasonal mean stream function 1975	- - - 48
18.	200 mb seasonal mean stream function 1976	- - - 49
19.	Sea surface temperature anomalies 1974-76	- - - - - 50
20.	Power spectral estimate plot of divergence in the eastern Pacific 1976	- - - - - 51
21.	Same as 20 except for western Pacific	- - - - - 52
22.	Power spectral estimate plot of $V^2$ in the eastern Pacific 1976	- - - - - 53
23.	Same as 22 except western Pacific	- - - - - 54

#### ACKNOWLEDGEMENTS

The financial support for the author's graduate program was provided by the United States Air Force through the Air Force Institute of Technology (AFIT). The author wishes to express his appreciation and thanks to Prof. C.-P. Chang and Prof. K.M.W. Lau for their guidance, encouragement and patience throughout this work. The 200 mb data were provided by the United States Navy's Fleet Numerical Weather Center and the satellite data were provided by the National Environmental Satellite Service/NOAA. This research was supported in part by NESS/NOAA under Contract ATM 77-14820.

## I. INTRODUCTION

Previous studies (Chang and Miller, 1977; Kanamitsu and Krishnamurti, 1978; Winston and Krueger, 1977; Bepristis, 1977) have analyzed upper air and satellite data in an effort to study the interannual variations of planetary-scale circulation over the tropics.

Chang and Miller (1977), in a spectral analysis of tropical easterly waves during the second half of 1972 and 1973, found considerable variation in the structure and properties of the disturbances between the two seasons. In the tropical eastern Pacific the 1972 season was characterized by abnormally large warm sea temperature anomalies, which had an effect of almost completely removing the normal zonal sea surface temperature gradient, while the 1973 season showed abnormally large cold sea surface temperature anomalies, which sharpened the gradient in the central Pacific. The periodicity of the waves in both seasons was found to be 4-5 days. However, the vertical structure and amplitudes of the waves exhibited marked differences.

An extensive study completed by Kanamitsu and Krishnamurti (1978) contrasted the 200 mb flow regimes during a drought year over central India and western Africa (1972) with those during a normal rainfall year over the same region (1967). Notable differences during the drought year (1972)

included the warm sea surface temperatures (Chang and Miller, 1977) which they related to a near doubling of typhoon days over the western Pacific and a shifting of the Tibetan High by some  $10^{\circ}$  eastward and equatorward.

Another study by Bepristis (1977) examined radiosonde data for 1974, 1975 and 1976 for the islands of Majuro, Ponape, Truk, Yap, Koror and in the tropical central and western Pacific. He also constructed sea surface temperature (SST) anomaly charts for the tropical Pacific (Figure 19) showing 1974 to be near normal, 1975 to be cold and 1976 to be warm. He found the thermal structure of the easterly waves was influenced more by the immediate upstream (about  $10^{\circ}$  longitude) SST than by the local SST.

A fourth study, that of Winston and Krueger (1977), introduced global patterns of outgoing long-wave radiation, albedo, absorbed solar radiation and net radiation derived from satellite observations. These patterns along with patterns of interannual differences in seasonal heating were examined for the three summers 1974-76 over the Eastern Hemisphere in relation to the variations in the summer monsoon and the major circulation features. Relating low values of outgoing long-wave radiation to cloudiness and rain they concluded 1975 was the strongest monsoon season, especially over the south and east. In 1974 the lowest outgoing radiation occurred in the area of NE India, Nepal and the Himalayas resulting in decreased cloudiness and rainfall over southern India. The 1976 monsoon had a

delayed start, was fairly active during July and August and receded somewhat early in September. A possible link relative to the delay of the monsoon in 1976 (and consequently weaker) compared to 1975 showed up in the equatorial Pacific eastward of New Guinea. In 1976 this area was characterized by decreases in long-wave radiation indicating more cloudiness and convection. Thus, the weaker monsoon was accompanied by major changes in the regions of condensation heating over the tropics. As we have already seen, (Kanamitsu and Krishnamurti, 1978), the increased cloudiness and convection in the eastern Pacific should indicate warmer sea surface temperatures in 1976 and this was verified (Bepristis, 1977).

The main objective of this work is to combine some of the parameters available from satellite data (Winston and Krueger, 1977) with other parameters available from 200 mb data (Kanamitsu and Krishnamurti, 1978) for the summers of 1974-76 to study interannual and intraannual fluctuations in the parameters  $U^2$ ,  $V^2$ , divergence, relative vorticity, infrared radiation and albedo. These parameters will be compared statistically to determine their inter-relationships within a particular system as well as between geographically separated systems.

## II. DATA AND ANALYSIS TECHNIQUE

### A. DATA SOURCES

#### 1. Satellite Data

Satellite data were obtained from the National Environmental Satellite Service/NOAA, which provided digitized information of infrared radiation (IR), available solar radiation ( $S_{av}$ ), and absorbed solar radiation ( $S_{ab}$ ) for the entire globe. The data are in radiative flux form, with values in watts per square meter. Area-averaged values were available on a 125x125 hemispheric grid with each grid value representing an area of approximately 150 km x 150 km.

#### 2. Upper Air Data

200 mb U-component and V-component data from analyzed wind fields were obtained from the Fleet Numerical Weather Center (FNWC), on their 49x144 mercator global band grid. This grid covers the area from 40° south to 60° north. The grid mesh distance at 22.5° north/south is 257 km.

### B. DATA PERIOD

All data were collected at 12 hour intervals for the period 16 May through 15 September 1974, 1975 and 1976 with the exception of  $S_{ab}$  and  $S_{av}$  which were only available once per day and IR,  $S_{ab}$  and  $S_{av}$  for the period 15-31 May 1974 (are not available).

### C. PARAMETERS CALCULATED

Seasonal mean fields at 200 mb for the following parameters were produced for the period 16 May - 15 September for each of the years 1974, 1975 and 1976.

#### 1. U-component

Seasonal mean U-component fields were produced on a 49x144 mercator global band grid by simply summing up values at each grid point for each time period and dividing by the number of time periods. See Figures 1-3 for 1974, 1975 and 1976 respectively.

#### 2. V-component

Seasonal mean V-component fields were produced on a 49x144 mercator global band grid by simply summing up values at each grid point for each time period and dividing by the number of time periods. See Figures 4-6 for 1974, 1975 and 1976 respectively.

#### 3. Divergence

Seasonal mean divergence fields were calculated on a 49x144 mercator global band grid from the seasonal mean U-component and seasonal mean V-component fields using equation (1) (Krishnamurti, 1970) with centered finite differencing. See Figures 7-9 for 1974, 1975 and 1976 respectively.

$$\text{Divergence} = \frac{\partial \bar{u}}{\partial x} + \frac{\partial \bar{v}}{\partial y} - \frac{\bar{v} \tan \phi}{a} \quad (1)$$

where  $a$  is the radius of the earth (=6371.229 km),  $(\bar{\quad})$  is the time-averaged mean and  $\phi$  the latitude.

#### 4. Relative Vorticity

Seasonal mean relative vorticity fields were calculated on a 49x144 mercator global band grid from the seasonal mean U-component and seasonal mean V-component fields using equation (2) (Krishnamurti, 1970) with centered finite differencing.

$$\text{Relative vorticity} = \frac{\partial \bar{v}}{\partial x} - \frac{\partial \bar{u}}{\partial y} + \frac{\bar{u} \tan \phi}{a} \quad (2)$$

See Figures 10-12 for 1974, 1975 and 1976 respectively.

#### 5. Stream Function

Seasonal mean stream function fields were calculated from the seasonal mean relative vorticity fields by solving the Poisson equation (3) (Krishnamurti, 1971), with boundary conditions given by equation (4) (Brown and Neilon, 1961).

See Figures 13-15 for 1974, 1975 and 1976, respectively.

$$\nabla^2 \bar{\psi} = \text{seasonal mean relative vorticity} \quad (3)$$

$$\psi_B : \frac{\partial \psi_B}{\partial S} = - V_n^{\text{obs}} \quad (4)$$

$$\psi_j' = \psi_j - \left(\frac{A}{N}\right)_j \quad j=1,2,---,N$$

where  $V_n$  = velocity component normal to the boundary

A = starting value minus value at the end of integration around the perimeter

N = number of distinct grid points around the boundary

## 6. Velocity Potential

Seasonal mean velocity potential fields were calculated from the seasonal mean divergence fields by solving the Poisson equation (5) (Krishnamurti, 1971).

$$\nabla^2 \bar{\chi} = \text{seasonal mean divergence} \quad (5)$$

$\bar{\chi}$  was assumed = 0 on the northern and southern boundaries of the grid and cyclic boundary conditions were used along the east-west side. See Figures 16-18 for 1974, 1975 and 1976 respectively.

### D. AREAS OF INTEREST

From each of the 200 mb seasonal mean U-component, V-component, divergence and relative vorticity fields, (Figures 1-12) three areas of interest were selected. From the divergence fields, the three areas were picked to represent regions of maximum time-averaged divergence and from the relative vorticity fields the three areas included the maximum negative vorticity centers. The three areas of interest on the U-component and V-component fields were picked as the regions of maximum North-South gradient of isopleths of stream function and velocity potential respectively. As a result of the selection criteria, areas may be different for different parameters and different seasons. Also, different areas may relate to the same system, e.g. easterly jets, anticyclones, western or eastern Pacific ITCZ, etc.

#### E. TIME SERIES PRODUCED

With the areas of interest defined and a time period of 16 May - 15 September in 12 hour intervals specified, 18 time series of area-averaged values were produced for each year. Three each from the U-component and V-component data where time series of the parameters  $U^2$  and  $V^2$  respectively were calculated instead of U and V as being more related to kinetic energy of the flow and their magnitudes less affected by the area-averaging process. There also were three of divergence and three of relative vorticity. The final six were from the digitized satellite data and were calculated over the same areas used for the divergence. Three of these were of area-averaged IR and three of area-averaged albedo using

$$\text{albedo} = \frac{S_{av} - S_{ab}}{S_{av}}$$

where  $S_{av}$  is the available solar energy and  $S_{ab}$  is the absorbed solar energy. A nine-point low pass filter was applied to all time series to remove the seasonal trends and eliminate periods in excess of 20 days.

#### F. STATISTICAL ROUTINE

The filtered time series were input to one of the routines of UCLA's Biomedical Computer Programs (BMD) Package (Dixon, 1976), BMD02T. Each time series was cross-correlated with all others. Parameters output included power spectrum estimates, co-spectra, coherence squares and cross covariances. A lag of 40 was chosen providing resolution of periods up to 20 days.

### III. RESULTS

#### A. COMPARISON OF THE THREE YEARS

In this section we shall examine the major differences in the large-scale 200 mb circulations during the years 1974-76. Winston and Krueger (1977) have already classified the three years relative to the Summer Asian Monsoon region as being dry (1974), normal (1975) and late starting/weaker (1976).

##### 1. Mean Circulations

Figures 1-3 show the fields of  $\bar{u}$  for the years 1974-76. The intensity of the tropical easterly jet over the Arabian Sea is nearly the same for all three years (around  $25 \text{ m s}^{-1}$ ) but the jet core is displaced about  $6^\circ$  north and  $7^\circ$  west in 1974 from the nearly coincident positions of 1975 and 1976. Winston and Krueger (1977) observed a similar displacement of the maximum cloudiness and precipitation areas in 1974. Kanamitsu and Krishnamurti (1978) observed a significant decrease in the intensity of the tropical easterly jet during a drought year over the monsoon region (1972).

Mid-latitude westerlies around  $40^\circ$  north are weakest in 1974 becoming stronger in 1975 and strongest as well as shifted eastward in 1976. This is consistent with an intensification and a shifting eastward of the Hadley-type

circulation in 1976 as indicated by the locations of the positive centers in the velocity potential (Figures 13-15), stronger 200 mb divergence (Figures 7-9) and increased poleward motion over the eastern Pacific. Also consistent with an eastward shift in the jet core is the weakening of the major 200 mb anticyclone in 1976 as indicated by the mean stream function (Figures 16-18).

In 1975, westerlies around  $20^{\circ}$  north over the mid Pacific are weakest and the equatorial easterlies are broken in the region  $140^{\circ}$ - $175^{\circ}$  west longitude. This is consistent with the southwest penetration of the mid Pacific trough (Figure 17) indicating upper-level cyclonic circulation in the mid Pacific. This shows up on the mean divergence field (Figure 8) as a strong divergent center and results in an intensified equatorial Walker circulation as seen from the mean velocity potential field (Figure 14). By contrast, 1976 has the strongest westerlies around  $20^{\circ}$  north in the mid Pacific. Looking at the stream function (Figure 18) we see ridging across the entire Pacific moving the mid Pacific trough to a position north and east of 1975. The appearance of a strong positive vorticity center (Figure 12) over this mid Pacific region indicates increased anticyclonic circulation, decreased divergence (Figure 9) and a strengthening of the easterlies forming a continuous band across the equatorial Pacific. This supports Kanamitsu (Kanamitsu and Krishnamurti, 1978) who related strong westerlies in this region to a drought year when comparing the years 1967 and 1972.

The region of poleward motion in the eastern Pacific (Figures 4-6) extends further west and is intensified in 1976 consistent with warmer sea surface temperatures and increased convection, latent heat release implied from the stronger upper-level divergence (Figures 7-9) found over these regions. In the eastern Mediterranean region, the poleward motion center is shifted southeastward and intensified in agreement with the southeastward movement of the main 200 mb anticyclone, the decrease in cloudiness and precipitation and a resulting increase in solar insolation.

## 2. Divergence

Figures 7-9 illustrate divergence for the years 1974-76. The strongest year 1976 has a nearly continuous band of divergence across the Pacific between  $5^{\circ}$  and  $10^{\circ}$  north indicating a much more active ITCZ probably as a result of the increased sea surface temperatures (Figure 19). This supports Winston and Krueger's (1977) areas of reduced long-wave radiation in 1976. The strong divergent center in the mid Pacific for 1975 reflects increased convection, latent heat release and stronger cross equatorial circulation as seen in the velocity potential (Figure 14). The divergence center associated with the major anticyclone is shifted northwest and is more intense in 1974. This agrees with the observed shift in cloud and precipitation patterns (Winston and Krueger, 1977) and reflects the increased insolation over a dry southern India.

### 3. Relative Vorticity

Figures 10-12 illustrate relative vorticity fields for the years 1974-76. The mid Pacific in 1976 shows a stronger area of relative vorticity indicating an increased anticyclonic circulation in the region of the observed increase in the easterlies. The strongest negative relative vorticity in all three years falls just north of a line connecting the vortices of the major anticyclone in the stream function (Figures 16-18).

### 4. Velocity Potential

Figures 13-15 show velocity potential for the years 1974-76. We can see the increased Hadley-type circulation in 1976 in the western Pacific resulting in an increase in the mid latitude westerlies at the northern extent of the Hadley cell. Note the shifting of this main divergent center eastward and southward in 1976 with an elongated center. Such a change perhaps reflects to a certain degree the warm sea surface temperatures across the Pacific and the increase in convective heat sources indicated by increased divergence to the east. We also see the east-west overturning between the main divergent center and eastern Africa is strongest in 1976. This indicates increased subsidence over eastern Africa resulting in decreased cloudiness and precipitation as observed by Winston and Krueger (1977). The changes in positions of the positive velocity potential centers can be interpreted as a shift eastward and intensification of the rising branch of the equatorial Walker cell. We also make

note of weaker westerlies in the mid latitudes in 1975. The convergent center at  $20^{\circ}\text{S } 50^{\circ}\text{E}$  is a consistent feature of all three years indicating cross equatorial flow.

#### 5. Nondivergent Circulations

The rotational part of the wind is computed from the stream function field. Figures 16-18 show the stream function field for the years 1974-76. The anticyclone over the monsoon region has a split center in all three years. This anticyclone is weakest in 1976 consistent with the shift eastward of the maximum westerlies to correspond to the northern extent of the increased Hadley circulation and decreased cloudiness over the Indian subcontinent. Along with the stronger mid latitude westerlies in 1976 there is ridging from the anticyclone nearly all the way across the Pacific. This ridging forces the mid Pacific trough to a position north and east of its 1975 location increasing the anticyclonic circulation in the mid Pacific and allowing the easterlies to dominate the equatorial Pacific.

#### B. POWER SPECTRA

The power spectral estimates are tabulated in Table I which shows the number of areas of each parameter that had a peak period within the range shown at the left. Thus, the number 3 indicates all three areas selected for that parameter in that year showed a peak period within the range listed and a 2 indicates that 2 of the 3 areas selected had a tendency for a peak period within the range listed, etc.

YEAR	PERIOD (DAYS)	U <sup>2</sup>	V <sup>2</sup>	δ	ξ	IR	ALB EDO
1974	3-4	3	3	3	3	3	2
	5-7	2	2	3	1	3	3
	> 8	1	0	0	0	0	0
1975	3-4	3	3	*	*	*	2
	5-7	2	2	*	*	*	3
	> 8	1	0	0	2	0	0
1976	3-4	3	3	3	3	3	2
	5-7	1	2	2	3	1	1
	> 8	1	1	0	2	1	1

\* indicates predominant period was  
4-5 days

Table I. Power Spectral Estimates

There was a strong diurnal cycle in the IR but periods less than 3 days have not been included. Note the predominance of the 3-4 day periodicity in 1974 and 1976. The predominant period in 1975, considered the normal monsoon season, was in the 4-5 day range. A secondary period in the 5-7 day range also shows up well in 1974 and 1976 while the trend in 1975 appears to have been toward a mean 4-5 day period. In 1976, the most active eastern Pacific year, there were more occurrences of a longer (greater than 8 day) period. This season was characterized by a more active ITCZ region and warmer sea surface temperatures across the Pacific equatorial regions (Bepristis, 1977). Sample plots of power spectral estimates are shown in Figures 20-23. Figures 20 and 21 are for the maximum time-averaged divergence areas in the eastern and western Pacific (1976) respectively. Figures 22 and 23 are for the maximum time-averaged  $V^2$  in the eastern and western Pacific (1976) respectively. Figures 20 and 21 show a maximum peak in the 3 to 4 day range and Figure 20 has a secondary peak in the 5 to 7 day period. Figure 22 has a maximum peak in the 5 to 7 day range with secondary peaks in the 3-4 day and greater than 8 day range while Figure 23 has a 3-4 day period.

### C. COHERENCE SQUARES

In this section we will be concerned with three things. First, we will summarize the relationships of the parameters whose areas fall within the monsoon system. Secondly, we

will look at the relationship of areas within the mid to eastern Pacific and finally the relationships existing between the mid to eastern Pacific and the monsoon areas. Results are tabulated in Tables II-IV for the monsoon system (74-76), the mid to eastern Pacific system (74-76) and relationships between the monsoon and mid to eastern Pacific systems respectively. An entry in the table indicates the two parameters are correlated with at least a 95% level of confidence. The period at which this correlation exists is given on the left of the table in days and the phase of the transfer function given in parts of a circle in the entry itself. From the table it is obvious we do not consider correlations for periods less than 4 days (or more than 20 by virtue of the filter used).

#### 1. Monsoon System Relationships

Within the monsoon region, 1974 shows the best correlation of the parameters, mostly at the 99% confidence level. The divergence corresponded well with the  $U^2$  parameter as well as with IR and albedo. The  $V^2$  parameter showed a strong correlation to  $U^2$  and albedo. The dry year 1976 was next in terms of correlation of parameters, mostly at the 95% confidence level. Here, the divergence showed a good correlation to the  $U^2$ , IR and albedo parameters. The normal year, 1975, showed a correlation of divergence to IR and albedo parameters and in  $U^2$  to albedo. The area of relative vorticity that fell within this region in each of the three years showed no correlation to other parameters

DAYS	1974					1975					1976								
	U <sup>2</sup>	V <sup>2</sup>	δ	ξ	IR	ALB	U <sup>2</sup>	V <sup>2</sup>	δ	ξ	IR	ALB	U <sup>2</sup>	V <sup>2</sup>	δ	ξ	IR	ALB	
4-6		-.07													-.07				
8-10												.28							
12			.34			.39						.32							
4-6						-.01													
8-10						.04													
12						-.05													
4-6						.01						-.04							.10
8-10						.07											.39		-.07
12						.46						.46							-.11
4-6																			
8-10																			
12																			
4-6						.50						-.47							.48
8-10						-.49						.47							.50
12						-.48						.50							.49

Table II. Coherence Squares Monsoon System





at the 95% or greater level. Other than the close relationship of infrared radiation, albedo and divergence which were all calculated over the same areas, there does not appear to be any pattern to the correlations between the parameters or the periods within the parameter.

## 2. Mid to Eastern Pacific System Relationships

In this region, 1976 showed the best results in correlation of the parameters. This was probably to be expected since this was the strongest and most active year in the eastern Pacific. Once again the divergence showed a strong relationship to the IR and albedo parameters and also to  $V^2$ . In 1974, only two parameters had areas of interest within this region (relative vorticity and  $V^2$ ) and they showed a good correlation. Surprisingly, in 1975 there were five parameters with areas of interest within this region but there were no correlations among them at the 95% level. Comparing the periods and phase relationships of the parameters in Table III that are also in Table II we see the periods are the same but the mid to eastern Pacific system is generally more out of phase. Year to year comparisons of periods and phase in the mid to eastern Pacific are not possible due to the lack of correlations in the years 1974 and 1975.

## 3. Inter-System Relationships

Because nearly all areas of interest chosen in 1974 fall within the monsoon region, it is impossible to obtain inter-system relationships for that year. Significant

correlations between the mid to eastern Pacific region and the monsoon system exist in both 1975 and 1976. In each year the  $V^2$  parameter in the mid to eastern Pacific correlates well with the IR parameter in the monsoon region but the period and the phase are different. The normal season 1975 has the relative vorticity in the mid Pacific correlating well with  $V^2$ , IR and relative vorticity in the vicinity of the monsoon area. During the dry season 1976, we have the relative vorticity in the mid Pacific related to the  $U^2$  and albedo parameters in the monsoon region and IR in the mid Pacific related to the  $U^2$  parameter of the monsoon region.

While we were able to show some correlations, they certainly are not conclusive since the area selection criteria we used did not guarantee that we would be calculating all parameters in both the mid Pacific and the monsoon regions. We feel more meaningful results can be obtained in future studies with more attention given to area selection.

#### IV. CONCLUSIONS

In this study of the interannual variations of the tropical atmospheric circulations we have seen that in an anomalously warm sea surface temperature year a stronger Hadley type circulation developed and was shifted eastward. This was consistent with increased convection associated with a more active ITCZ, increased latent heat release, increased divergence aloft, a northward transport of momentum with a corresponding increase in the mid latitude westerlies and increased poleward movement in the eastern Pacific. This in turn appears to weaken the influence of the mid Pacific trough increasing the anticyclonic circulation over the mid Pacific and strengthening the easterlies into a continuous band across the Pacific. This sequence of events parallels Bjerknes (1969) hypothesis. We have shown correlations do exist among parameters within the eastern Pacific and the western Pacific regions and also between the two regions. Since the best correlations occurred between parameters calculated over the same geographical area we feel more attention given to area selection would produce more meaningful results than by just sampling each parameter in each region.

1974 SEASONAL MEAN U-COMPONENT  
CONTOUR INTERVAL 5M/SEC

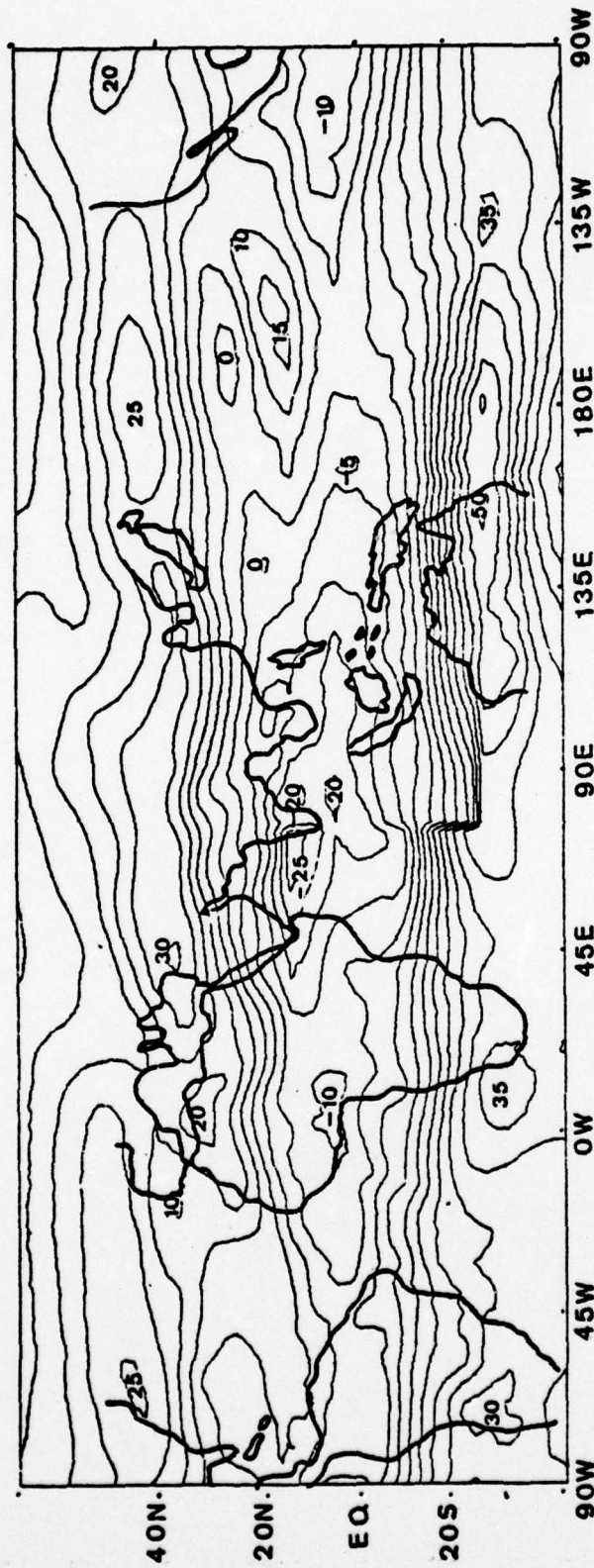


Figure 1. 200 mb seasonal mean U-component 1974.

1975 SEASONAL MEAN U-COMPONENT  
CONTOUR INTERVAL 5M/SEC

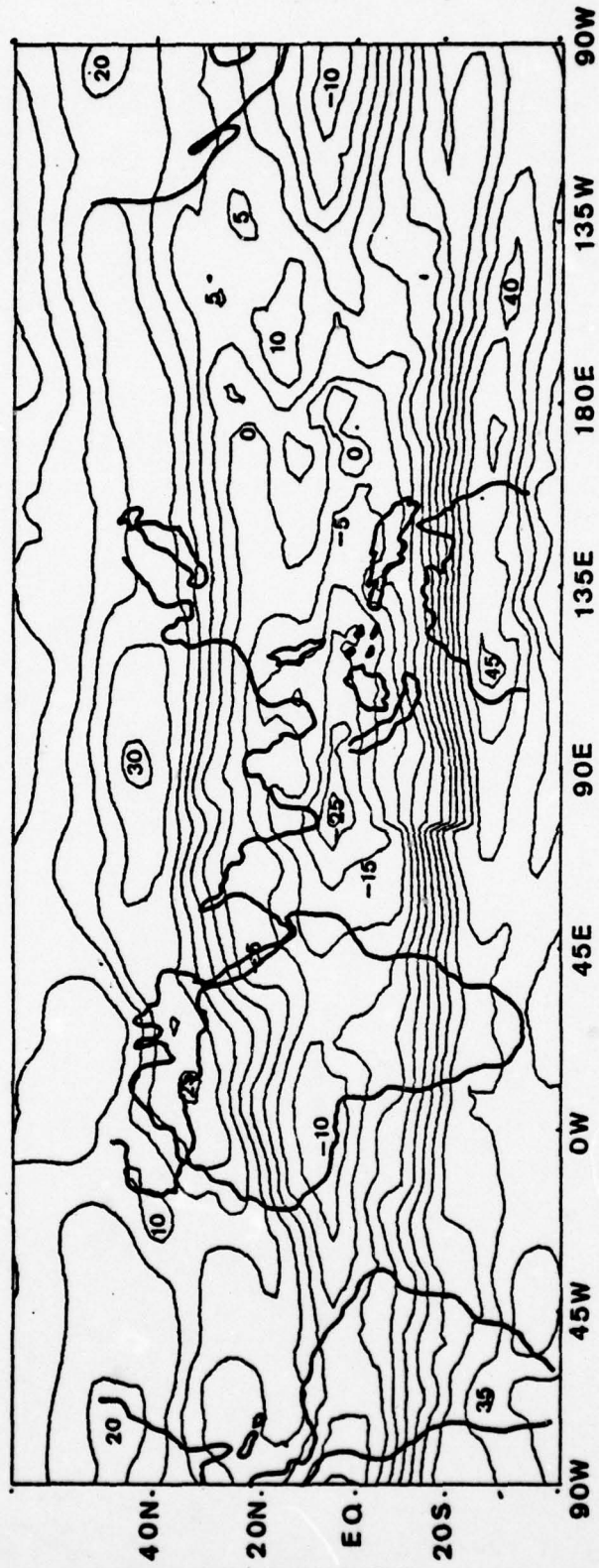


Figure 2. 200 mb seasonal mean U-component 1975.

1976 SEASONAL MEAN U-COMPONENT  
CONTOUR INTERVAL 5M/SEC

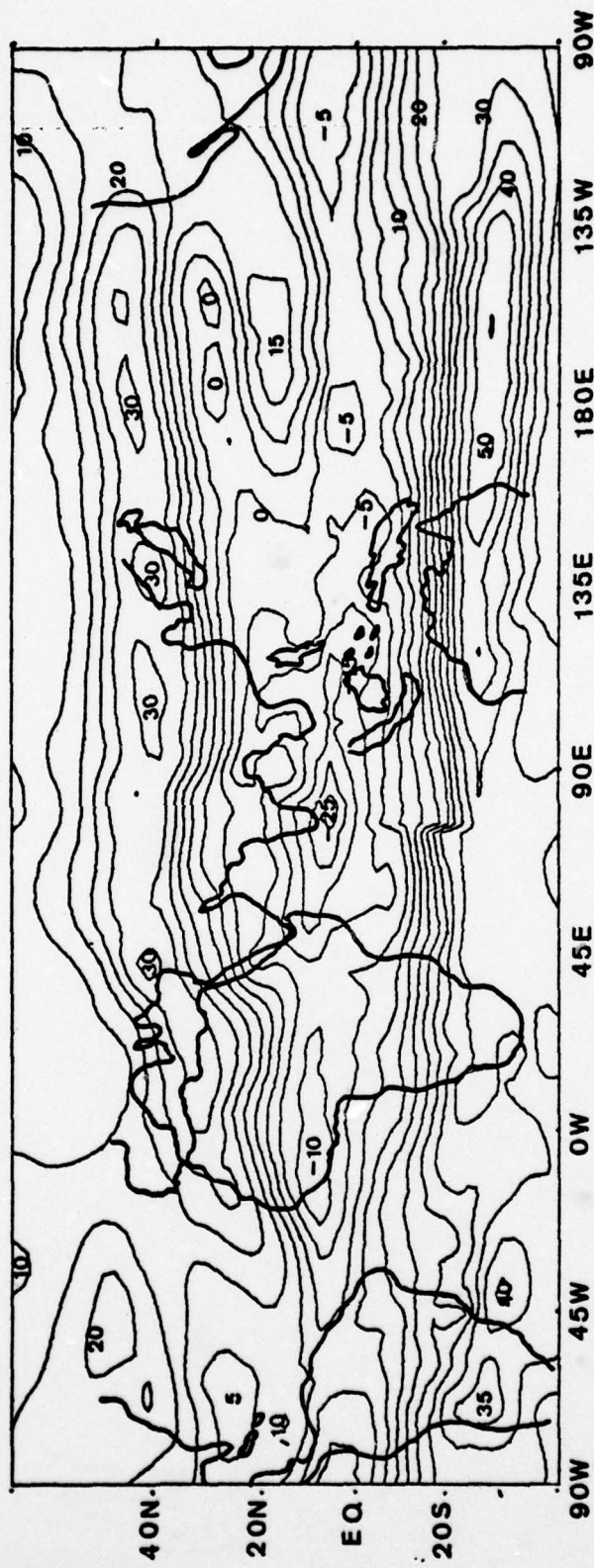


Figure 3. 200 mb seasonal mean U-component 1976.

1974 SEASONAL MEAN V-COMPONENT  
CONTOUR INTERVAL 3M/SEC

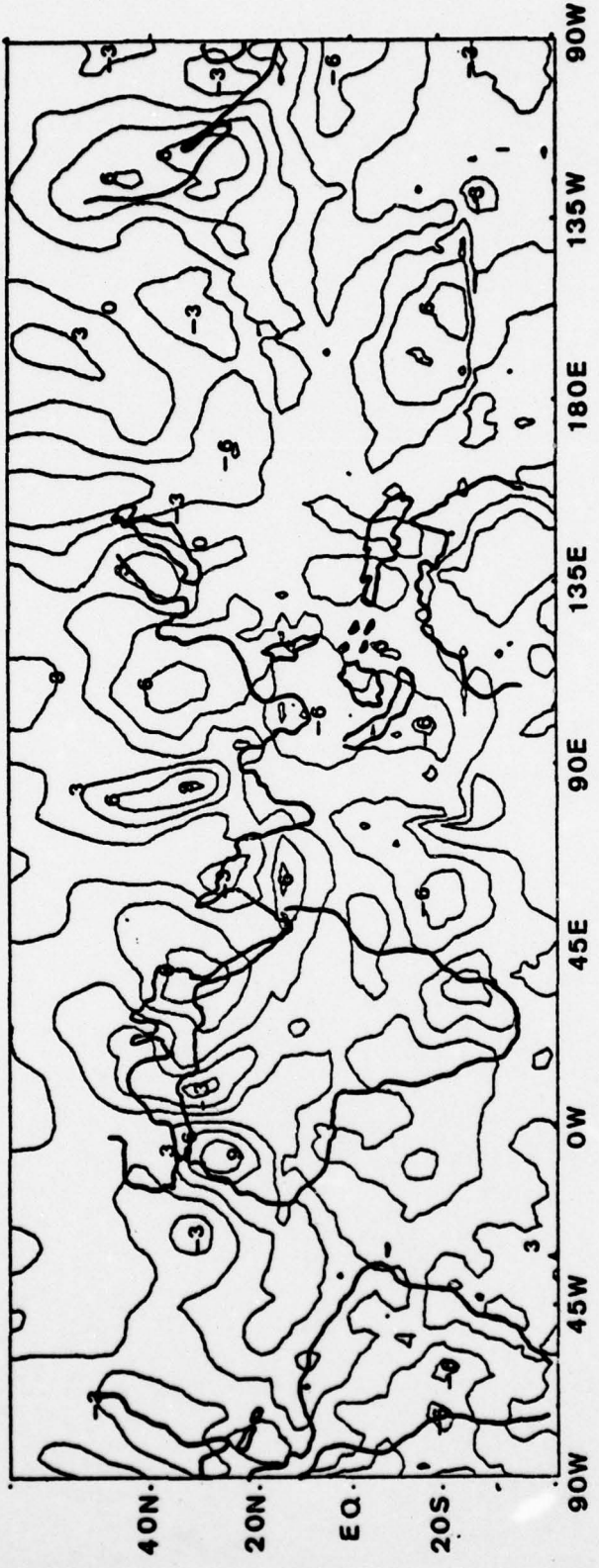


Figure 4. 200 mb seasonal mean V-component 1974.

1975 SEASONAL MEAN V-COMPONENT  
CONTOUR INTERVAL 3M/SEC

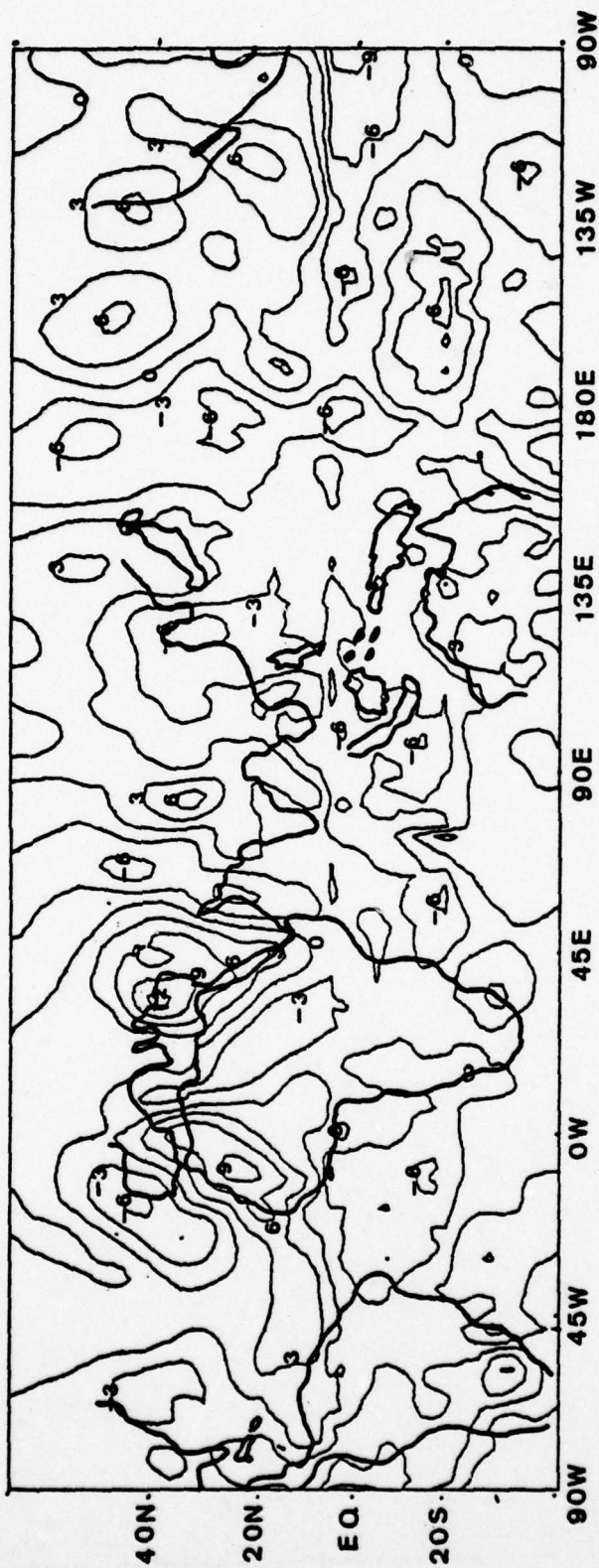


Figure 5. 200 mb seasonal mean V-component 1975.

1976 SEASONAL MEAN V-COMPONENT  
CONTOUR INTERVAL 3M/SEC

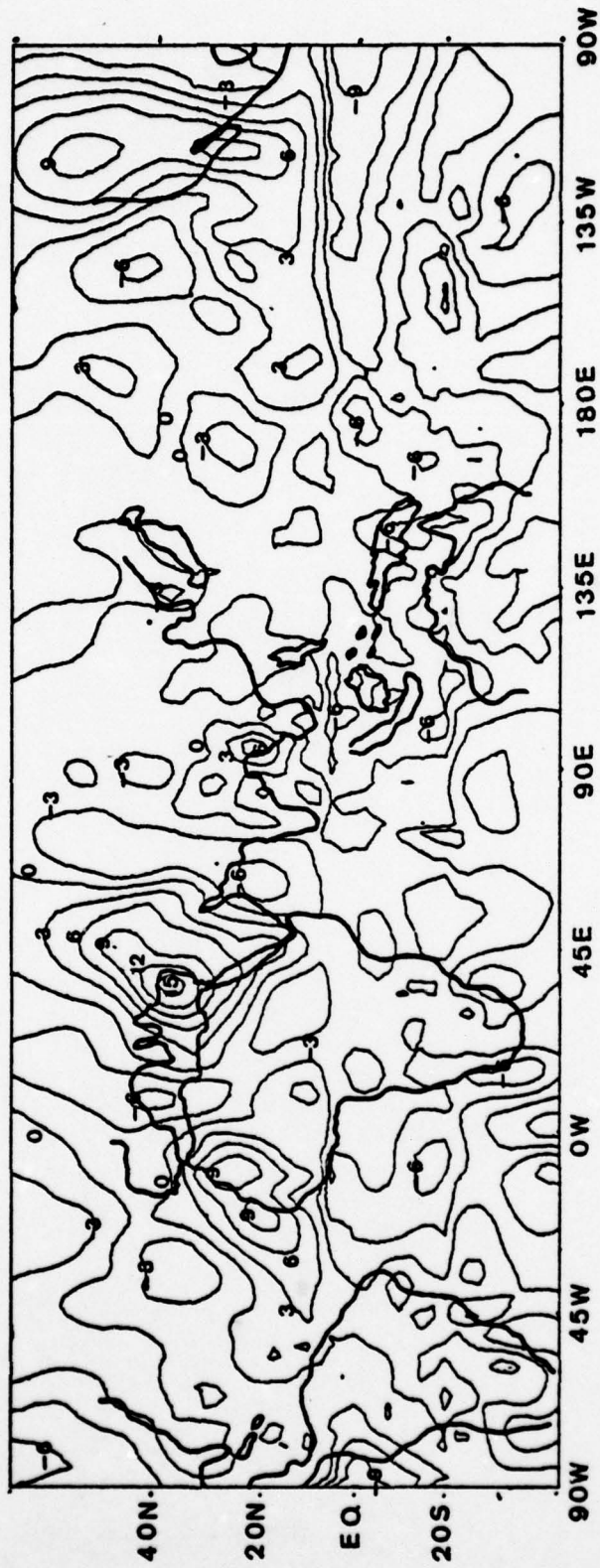


Figure 6. 200 mb seasonal mean V-component 1976.

1974 SEASONAL MEAN DIVERGENCE  
CONTOUR INTERVAL  $5 \times 10^{-6}$  M/SEC

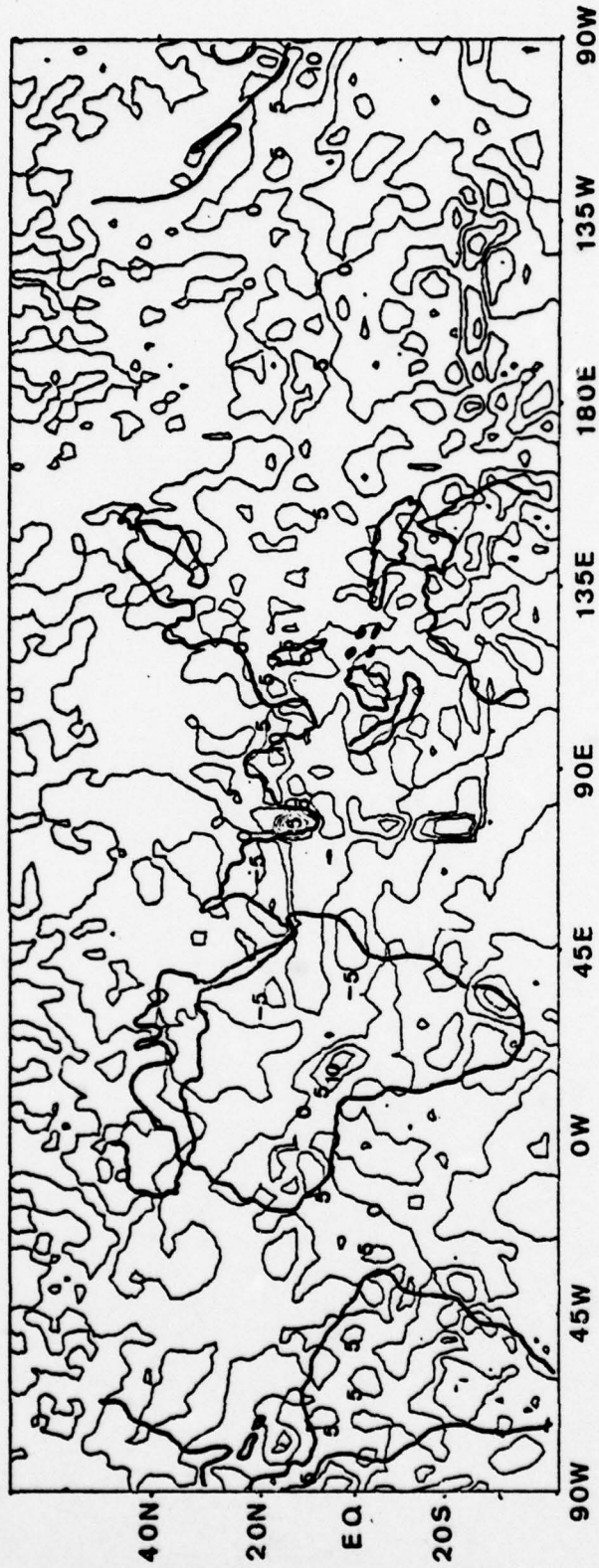


Figure 7. 200 mb seasonal mean divergence 1974.

1975 SEASONAL MEAN DIVERGENCE  
CONTOUR INTERVAL  $5 \times 10^{-5}$  M/SEC

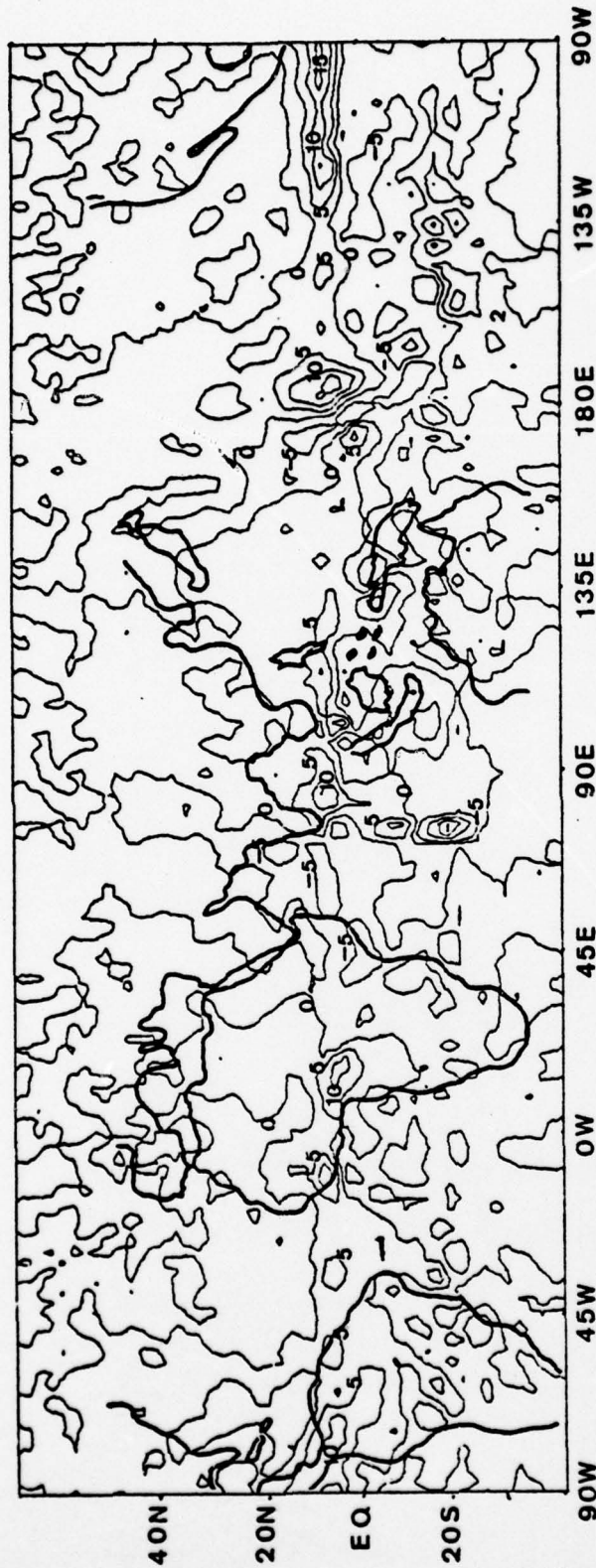


Figure 8. 200 mb seasonal mean divergence 1975.

1976 SEASONAL MEAN DIVERGENCE  
CONTOUR INTERVAL  $5 \times 10^{-5}$  M/SEC

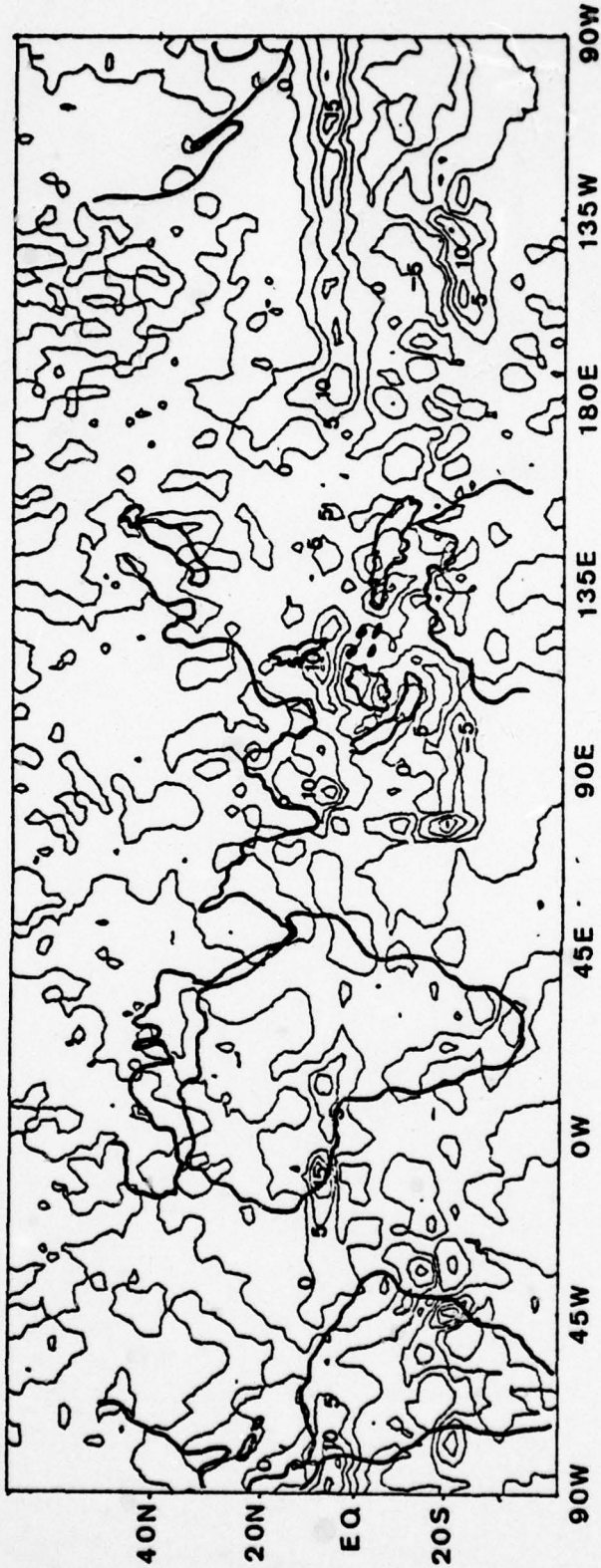


Figure 9. 200 mb seasonal mean divergence 1976.

1974 SEASONAL MEAN REL VORTICITY  
CONTOUR INTERVAL  $1 \times 10^{-4}$  / SEC

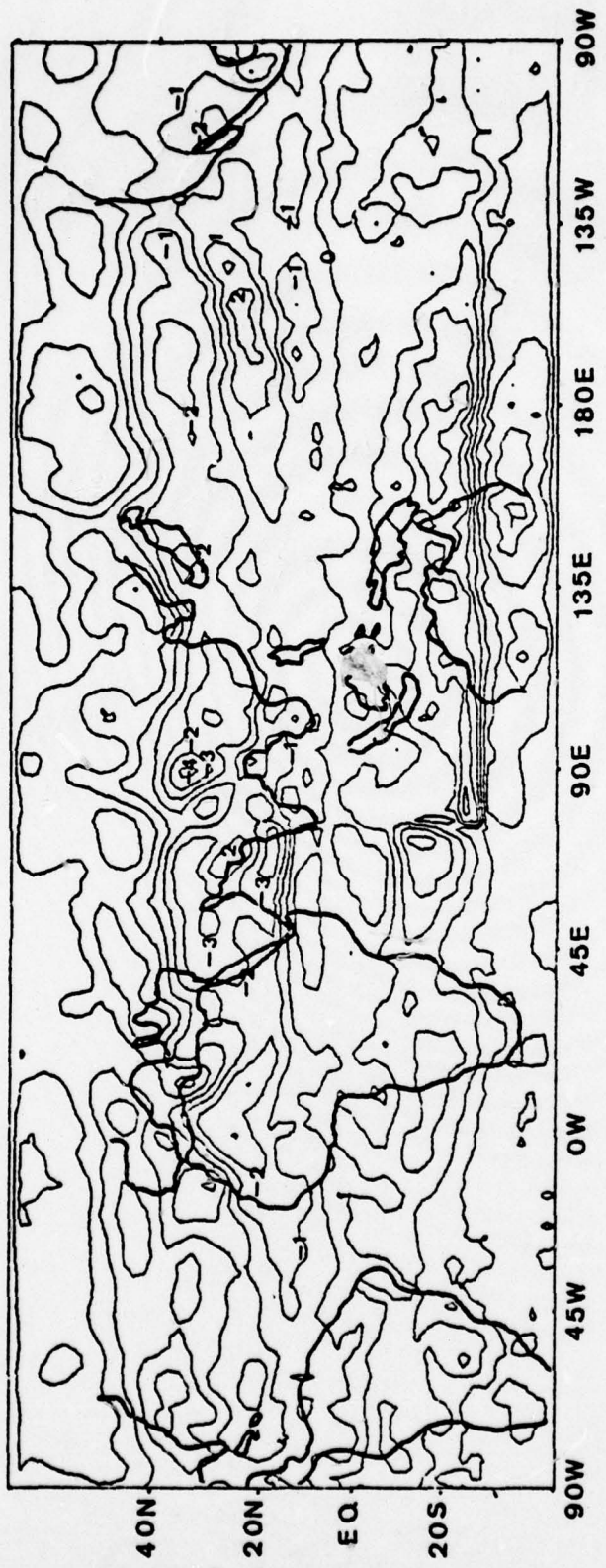


Figure 10. 200 mb seasonal mean relative vorticity 1974.

1975 SEASONAL MEAN REL VORTICITY  
CONTOUR INTERVAL  $1 \times 10^4$  /SEC

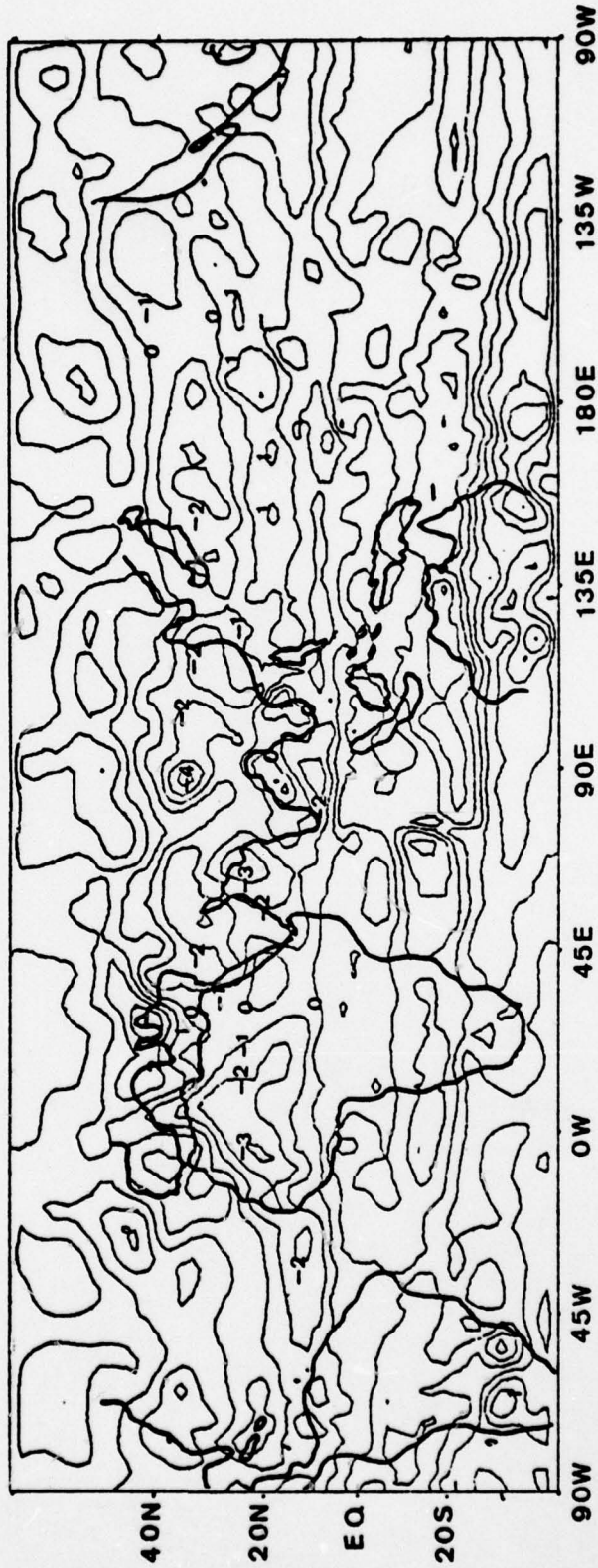


Figure 11. 200 mb seasonal mean relative vorticity 1975.

1976 SEASONAL MEAN REL VORTICITY  
CONTOUR INTERVAL  $1 \times 10^4$  / SEC

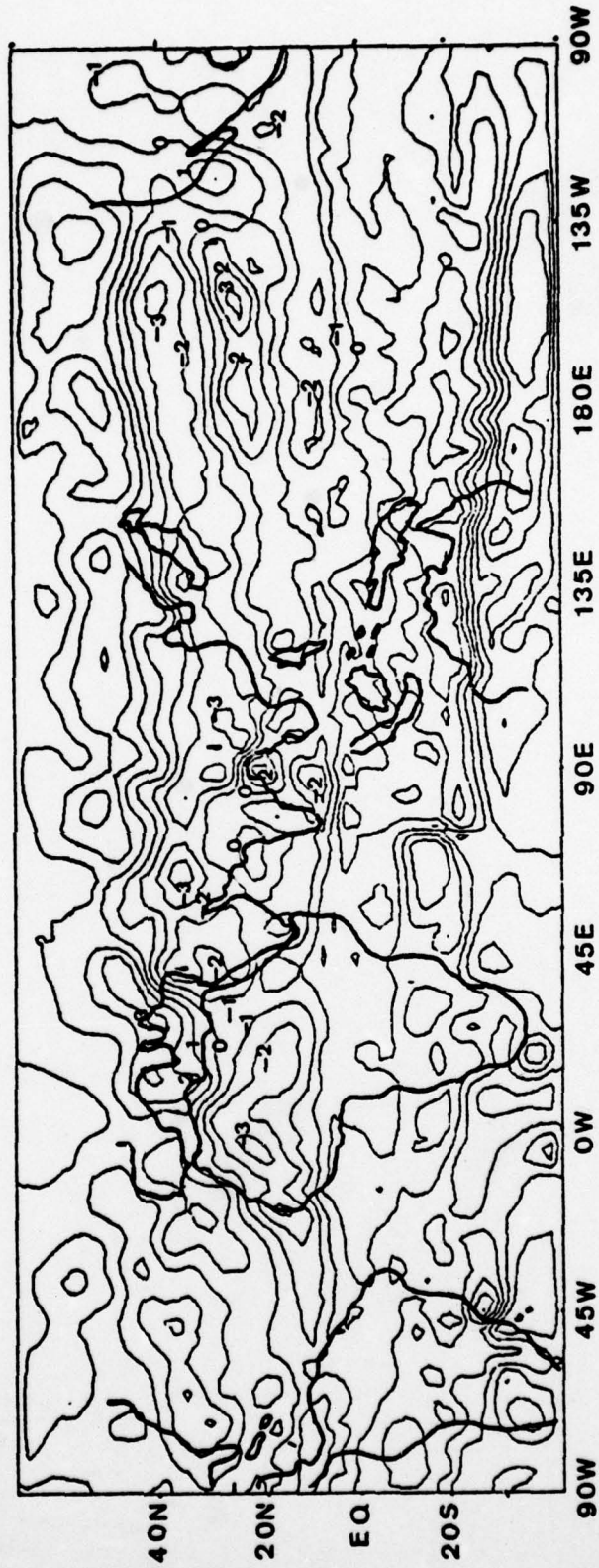


Figure 12. 200 mb seasonal mean relative vorticity 1976.

1974 SEASONAL MEAN VELOCITY POT  
CONTOUR INTERVAL  $1 \times 10^6 \text{ M}^2 / \text{SEC}$

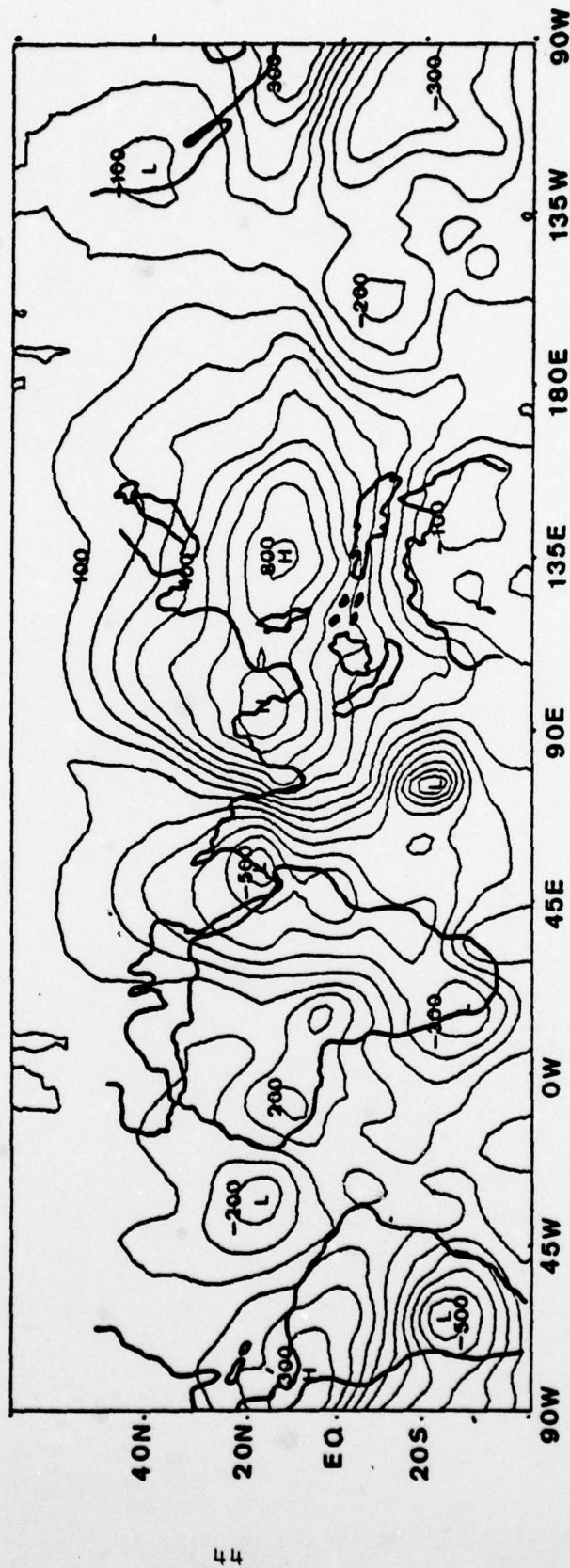


Figure 13. 200 mb seasonal mean velocity potential 1974.

1975 SEASONAL MEAN VELOCITY POT  
CONTOUR INTERVAL  $1 \times 10^6 \text{ M}^2/\text{SEC}$

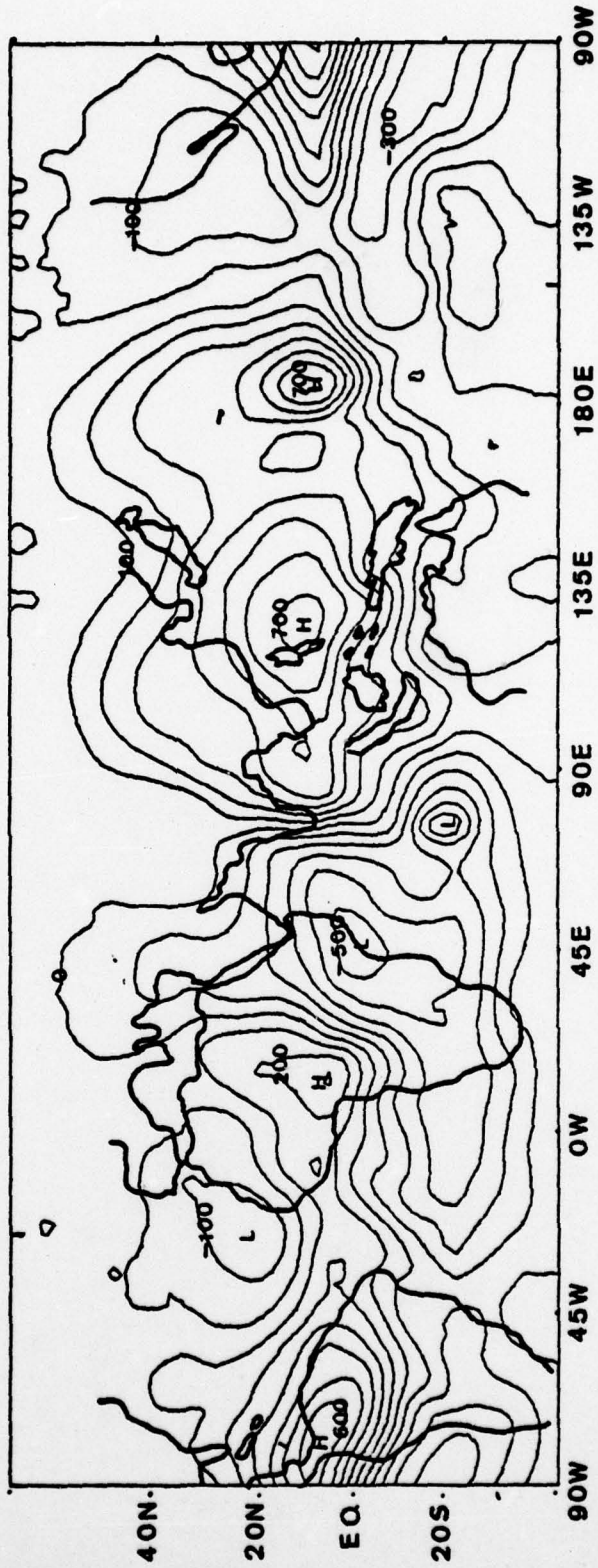


Figure 14. 200 mb seasonal mean velocity potential 1975.

1976 SEASONAL MEAN VELOCITY POT  
CONTOUR INTERVAL  $1 \times 10^6 \text{ M}^2 / \text{SEC}$

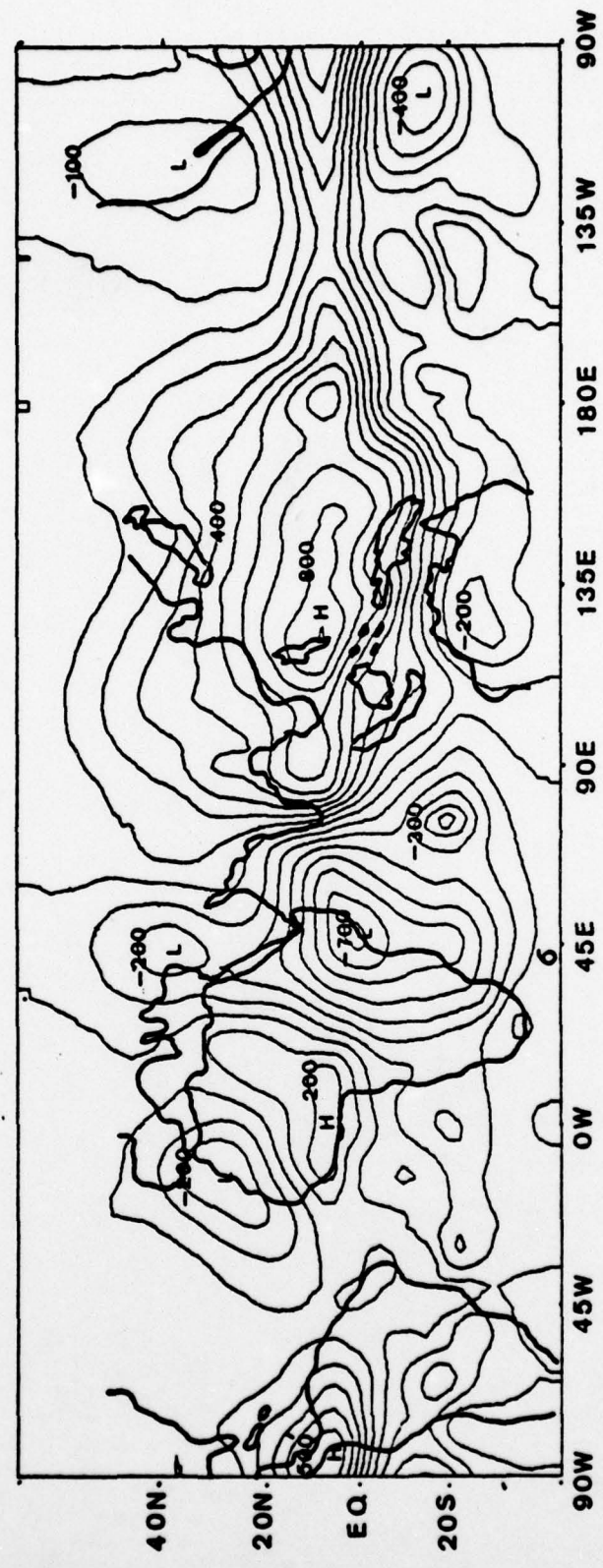


Figure 15. 200 mb seasonal mean velocity potential 1976.

1974 SEASONAL MEAN STREAMFUNCTION  
CONTOUR INTERVAL  $5 \times 10^6 \text{ M}^2 / \text{SEC}$

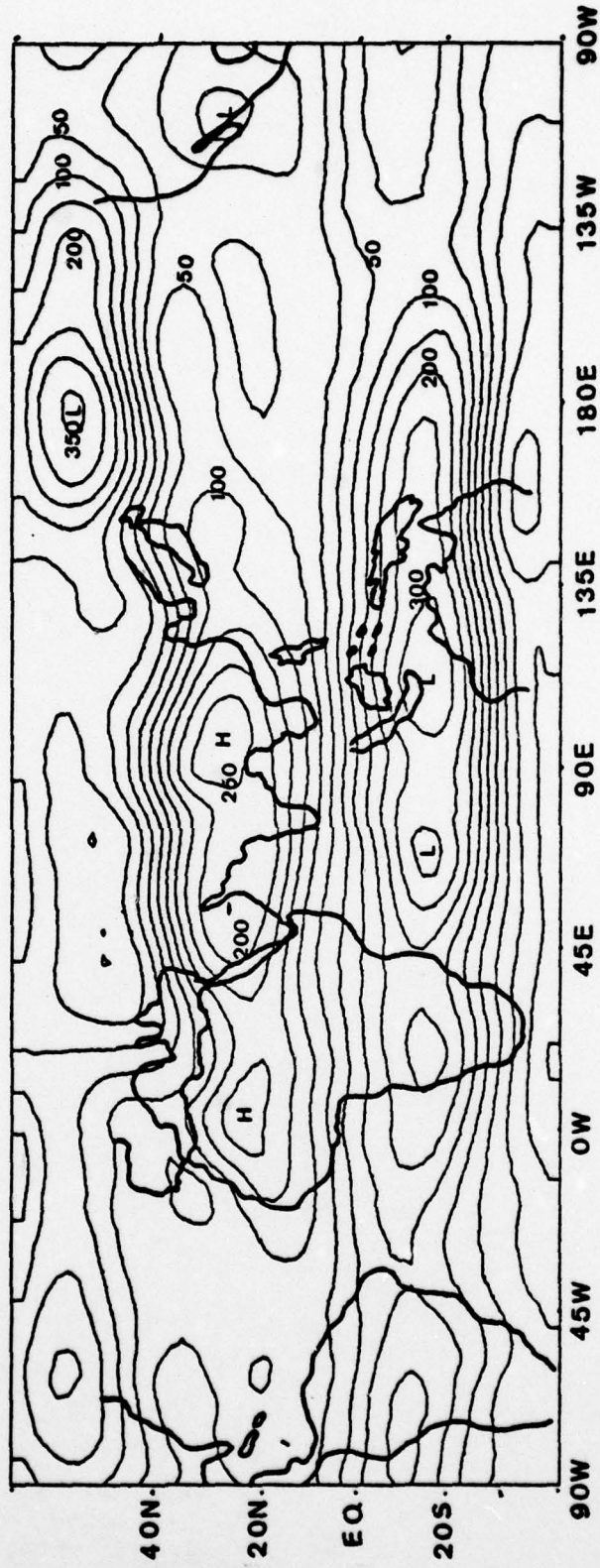


Figure 16. 200 mb seasonal mean stream function 1974.

1975 SEASONAL MEAN STREAMFUNCTION  
CONTOUR INTERVAL  $5 \times 10^6 \text{ M}^2/\text{SEC}$

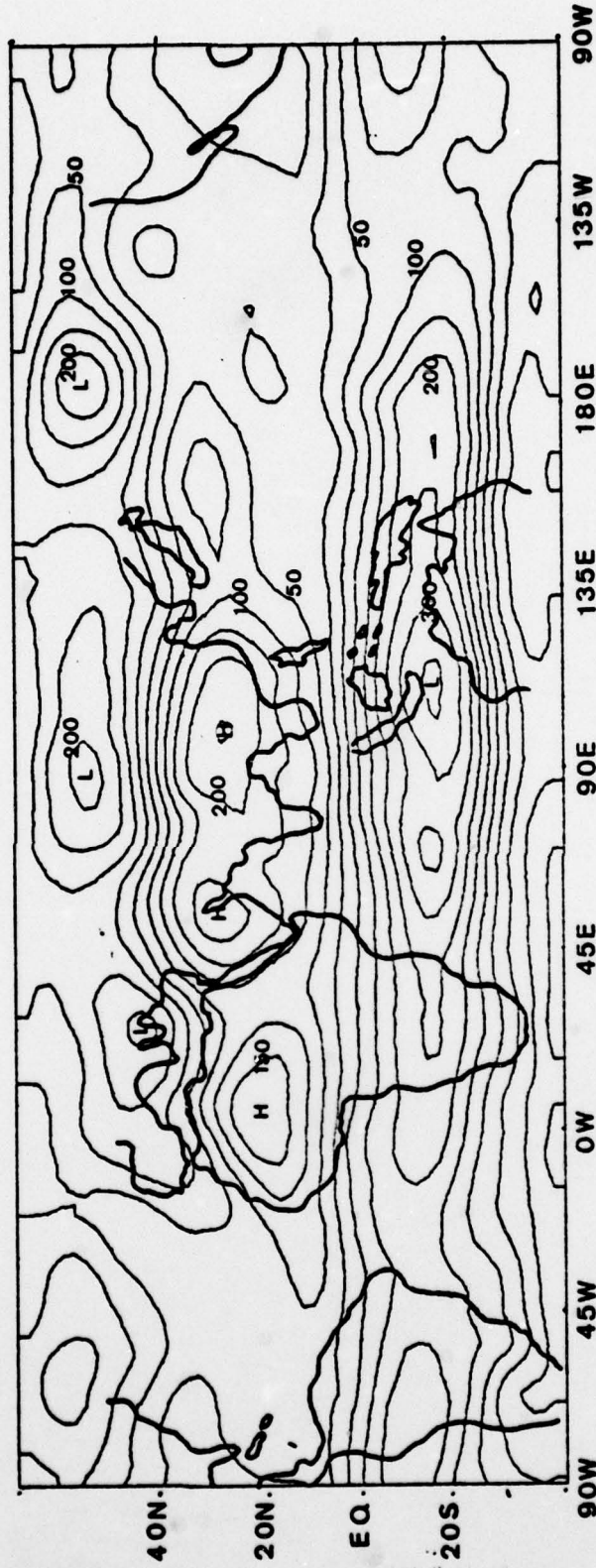


Figure 17. 200 mb seasonal mean stream function 1975.

1976 SEASONAL MEAN STREAMFUNCTION  
CONTOUR INTERVAL  $5 \times 10^6 \text{ M}^2 / \text{SEC}$

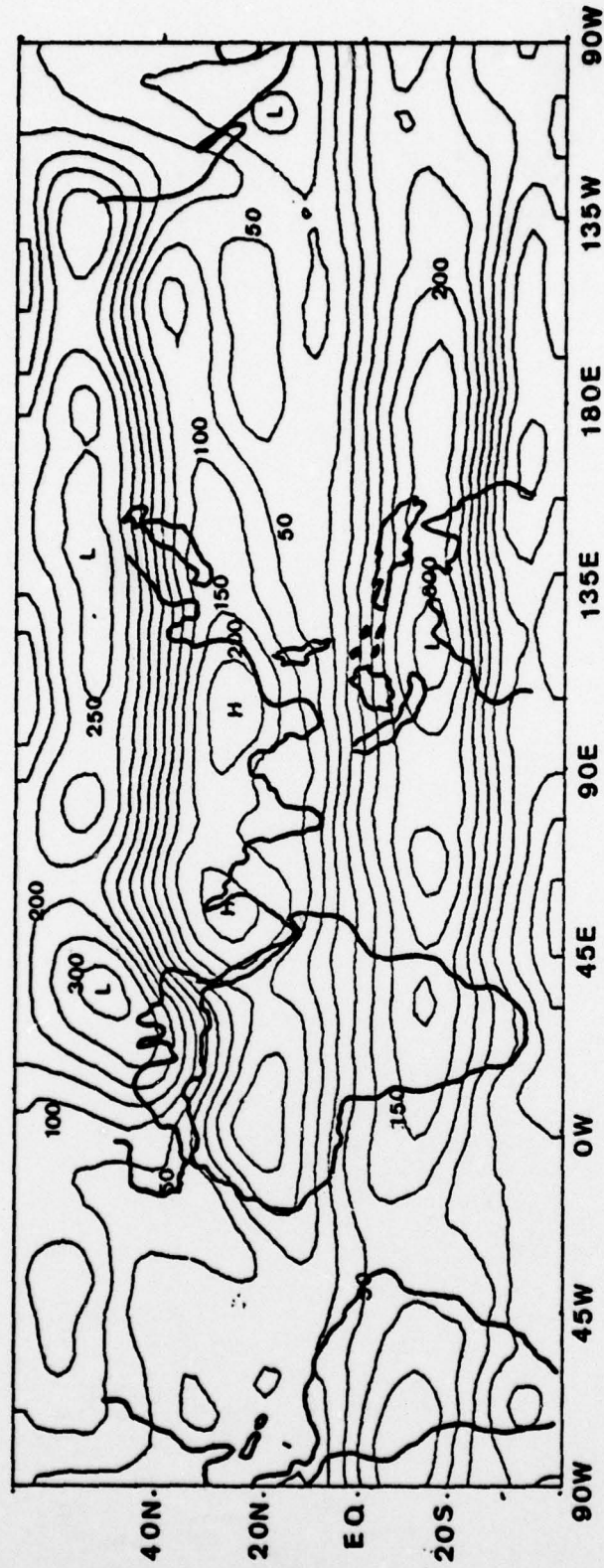


Figure 18. 200 mb seasonal mean stream function 1976.

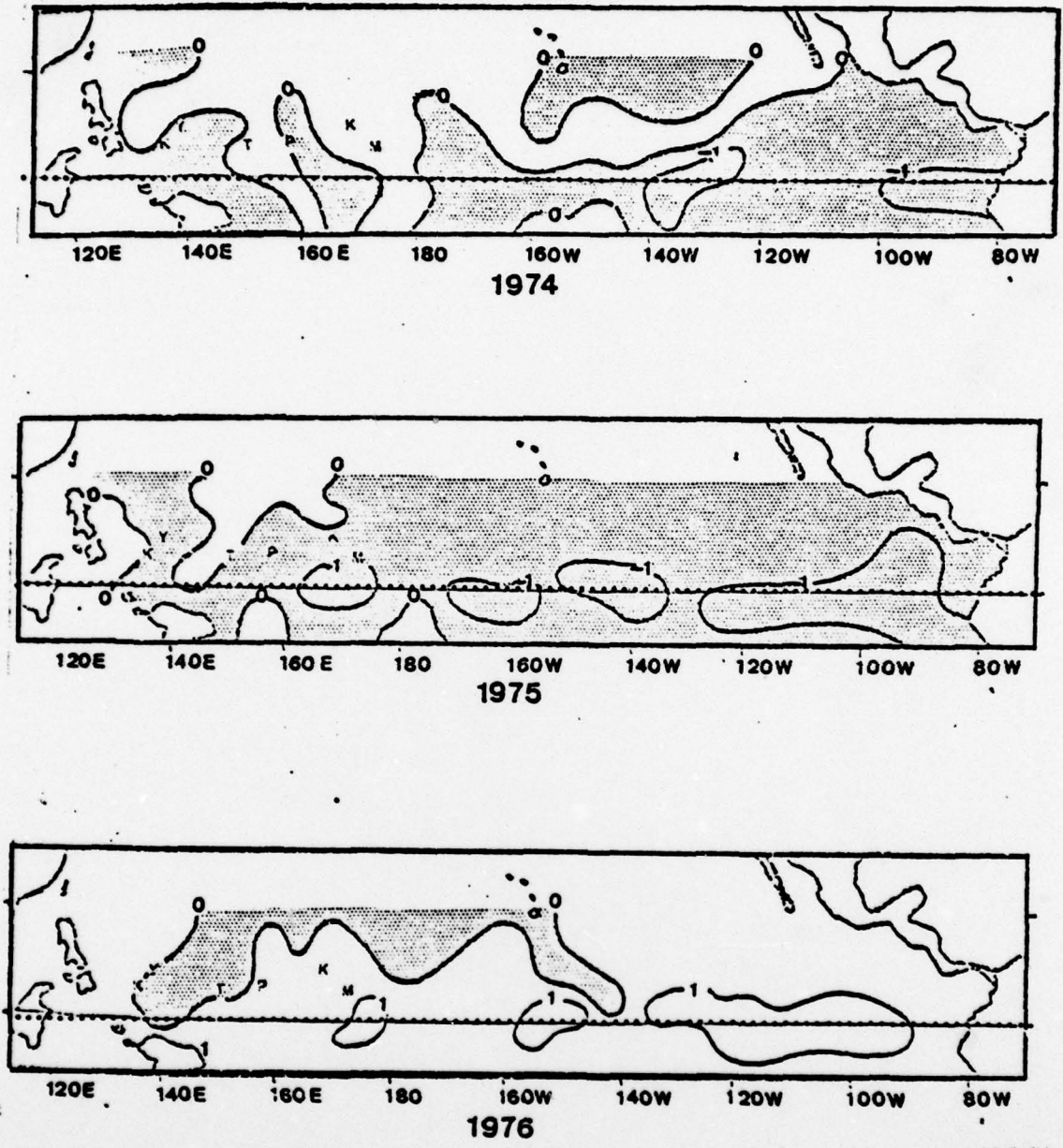


Figure 19. Sea surface temperature anomalies 1974-76.

GRAPH OF THE POWER SPECTRAL ESTIMATES OF SERIES 8 AGAINST FREQUENCY (CYCLES/ DAY)

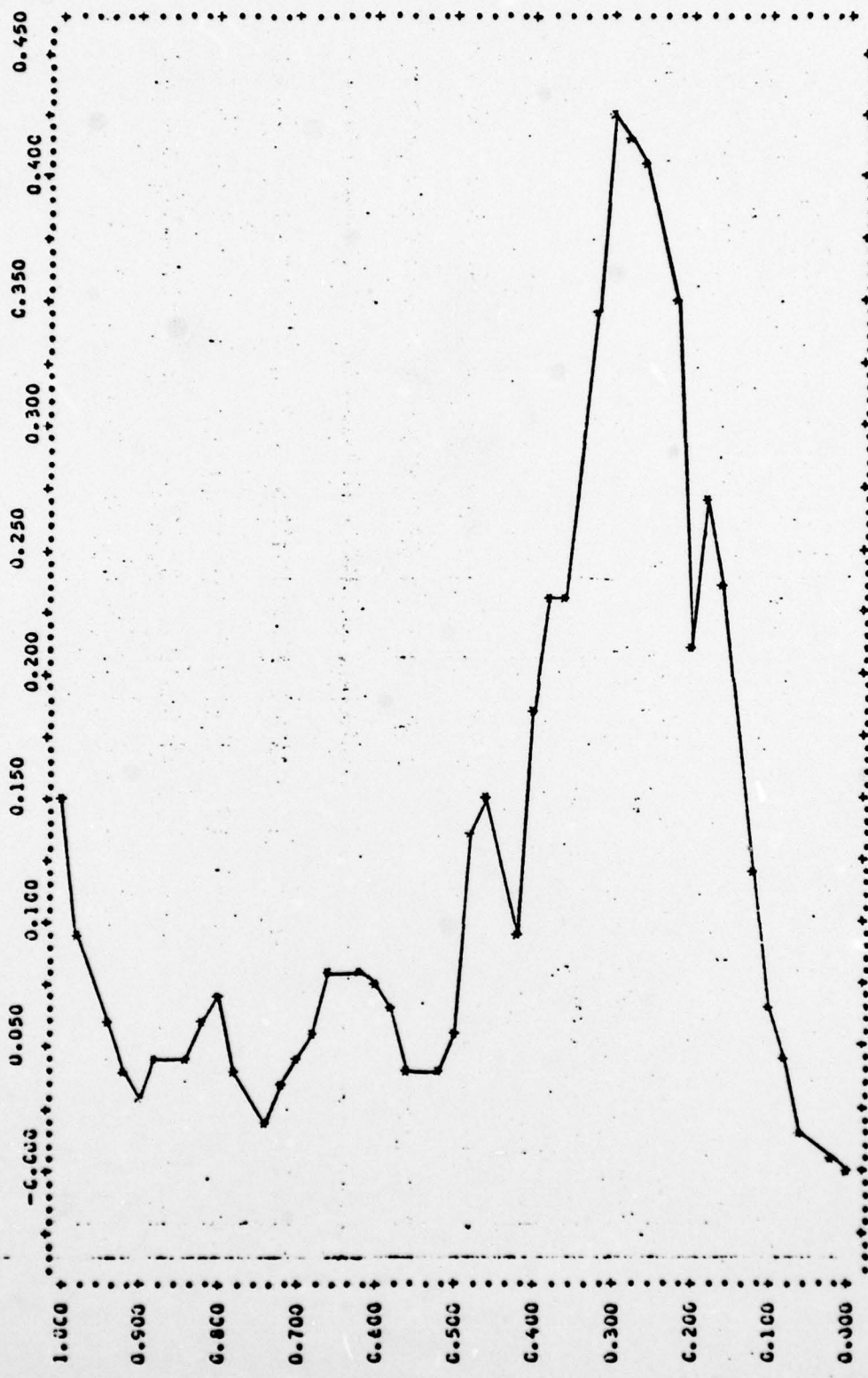


Figure 20. Power spectral estimate plot of divergence in the eastern Pacific 1976.

GRAPH OF THE POWER SPECTRAL ESTIMATES OF SERIES 7 AGAINST FREQUENCY (CYCLES/ DAY)

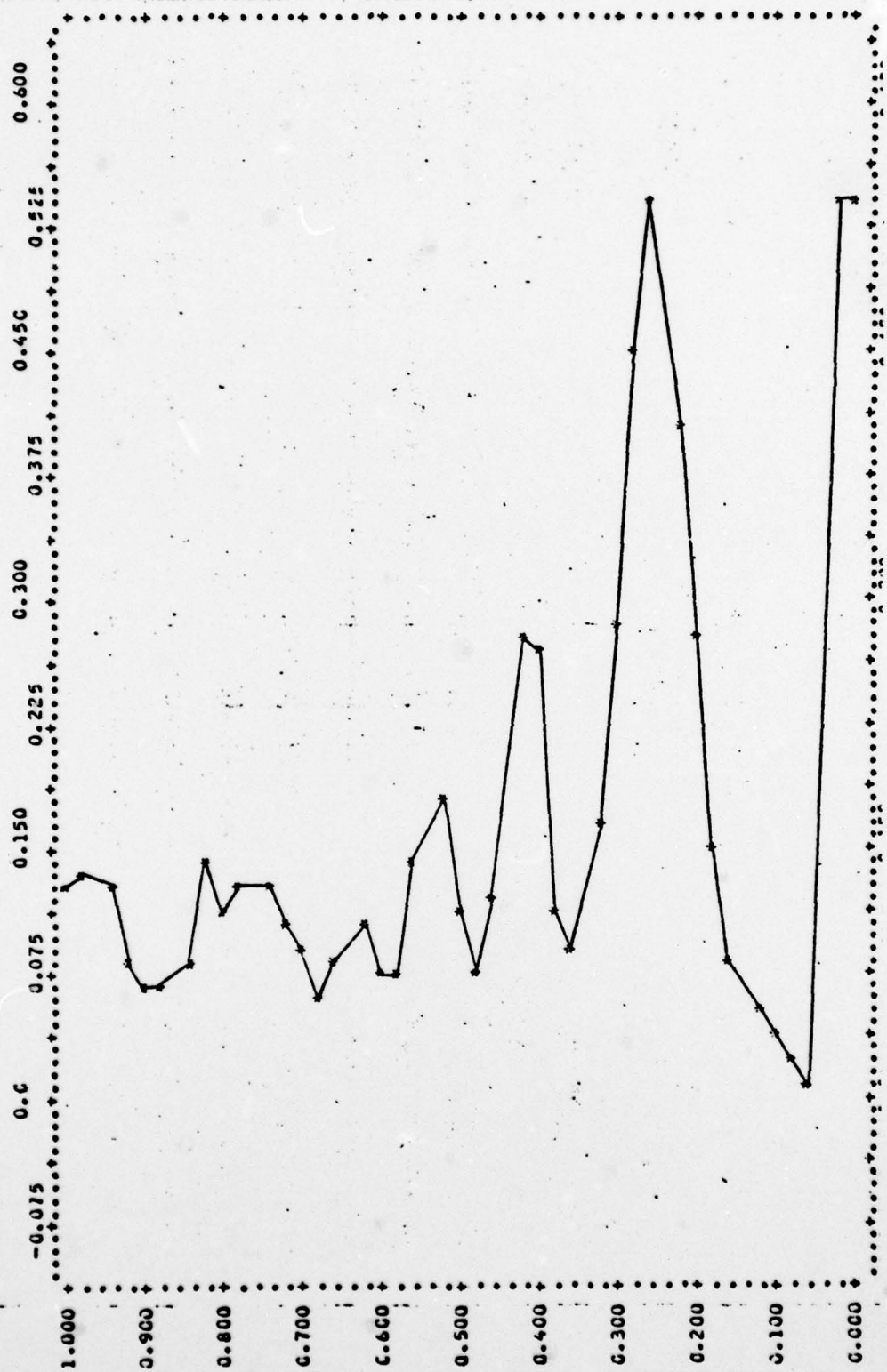


Figure 21. Same as 20 except for western Pacific.

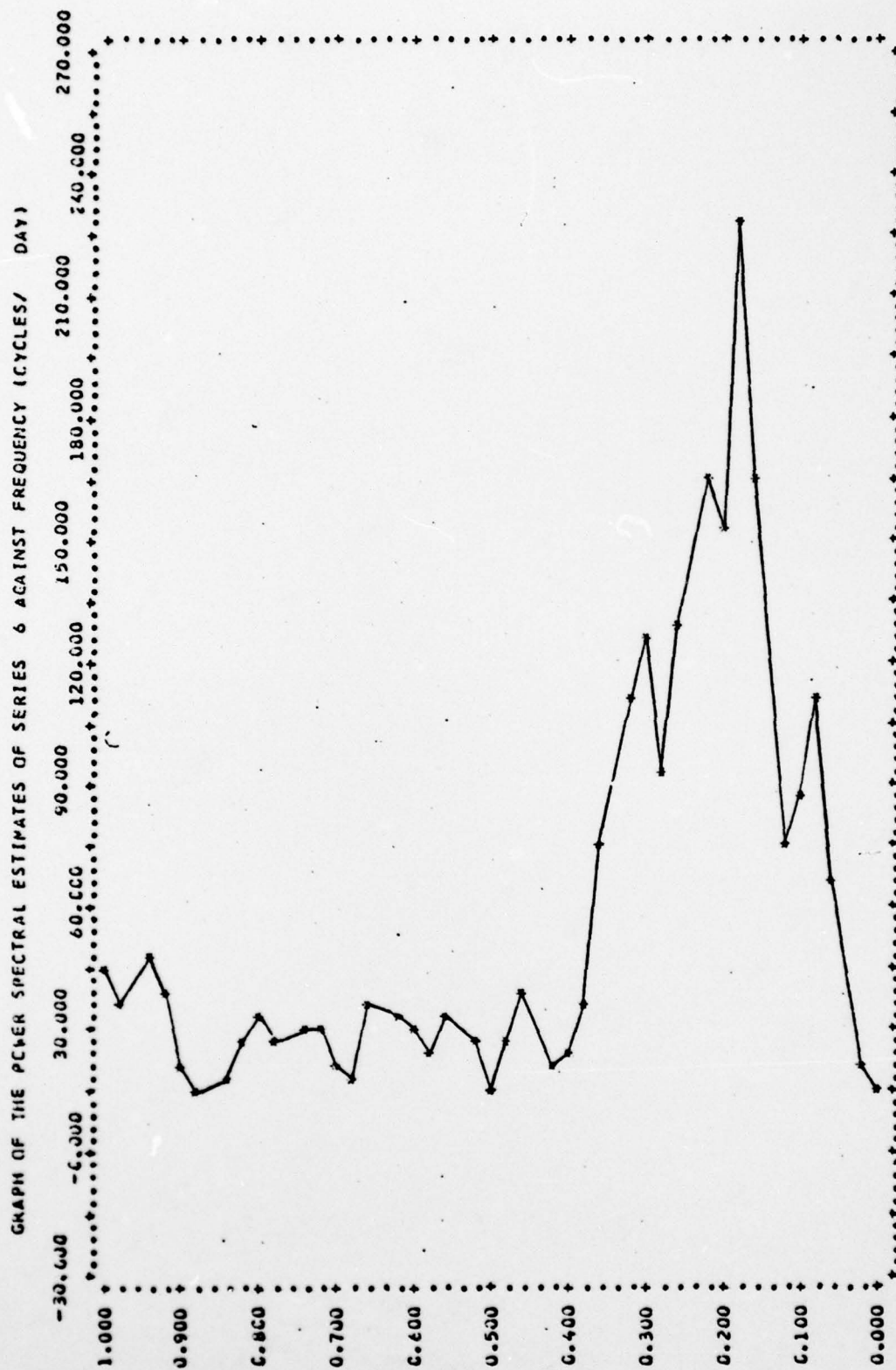


Figure 22. Power spectral estimate plot of  $V^2$  in the eastern Pacific 1976.

GRAPH OF THE POWER SPECTRAL ESTIMATES OF SERIES 4 AGAINST FREQUENCY (CYCLES/ DAY)

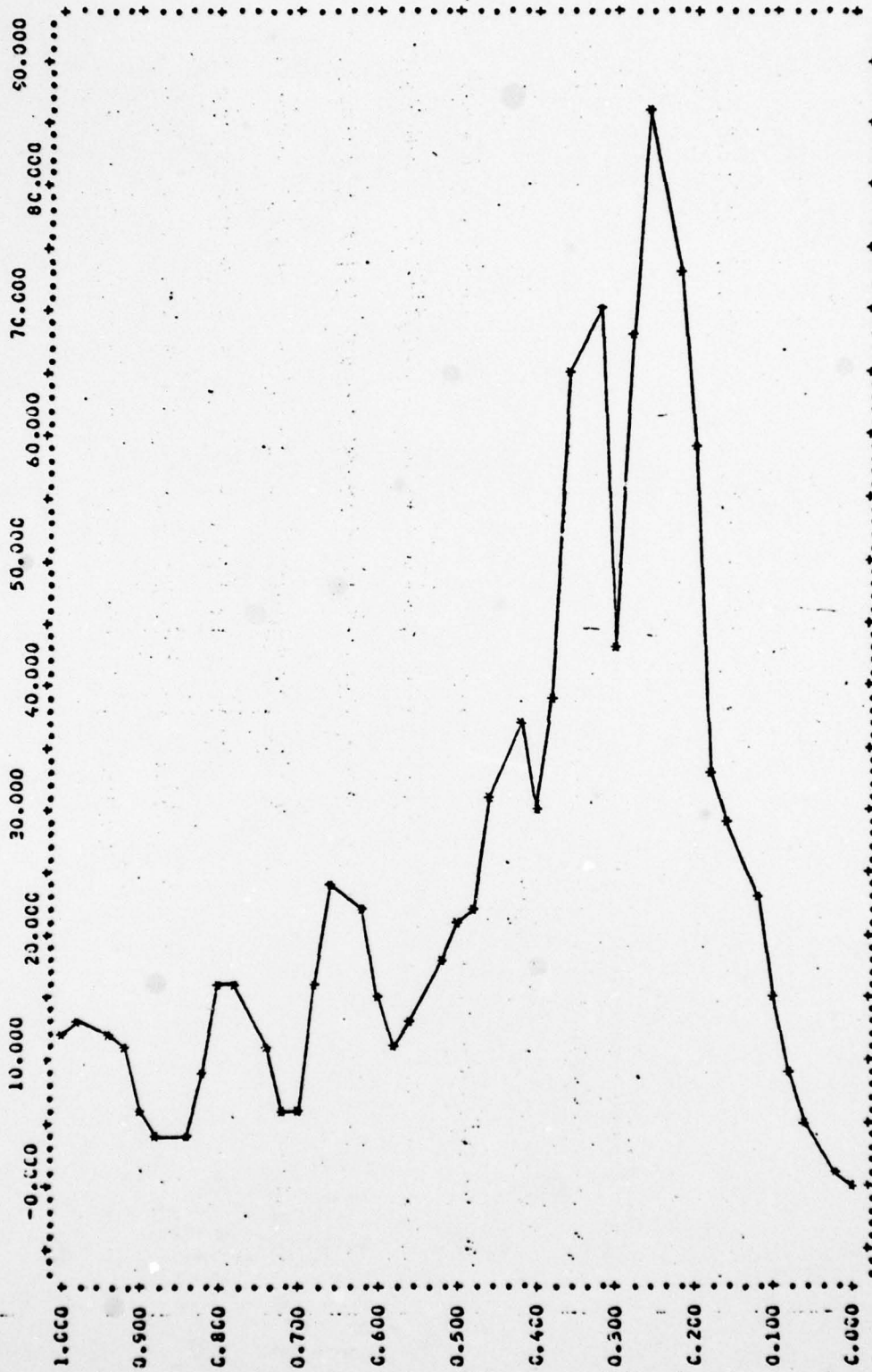


Figure 23. Same as 22 except western Pacific.

## LIST OF REFERENCES

- Beprestis, Donald J., 1977: Structure of Synoptic Scale Waves in the Tropical Pacific During July-December 1974-1976, Master's Thesis, Naval Postgraduate School, Monterey.
- Bjerknes, J., 1969: "Atmospheric Teleconnections from the Equatorial Pacific." Mon. Wea. Rev., 97, 163-172.
- Brown, J. and J. R. Neilon, 1961: "Case Studies of Numerical Wind Analysis." Mon. Wea. Rev., 89(3), 83-90.
- Dixon, W. J., 1976: BMD - Biomedical Computer Programs, University of California Press, Los Angeles, California, 773 pp.
- Kanamitsu, M. and Krishnamurti, T. N., 1978: "Northern Summer Tropical Circulations During Drought and Normal Rainfall Months." Mon. Wea. Rev., 106, 331-347.
- Krishnamurti, T. N., 1970: "Observational Study of Tropical Upper Tropospheric Motion Field During Northern Hemisphere Summer." Report No. 70-4, Department of Meteorology, Florida State University, Tallahassee, 73 pp.
- \_\_\_\_\_, 1971: "Tropical East-West Circulations During the Northern Summer." J. Atmos. Sci., 28(8), 1342-1347.
- Winston, J. S. and Arthur F. Krueger, 1977: "Diagnosis of the Satellite - Observed Radiative Heating in Relation to the Summer Monsoon." Pageoph, 115, 1131-1144.

INITIAL DISTRIBUTION LIST

	No. Copies
1. Defense Documentation Center Cameron Station Alexandria, Virginia 22314	2
2. Library, Code 0142 Naval Postgraduate School Monterey, California 93940	2
3. Dr. G. J. Haltiner, Code 63Ha Chairman, Department of Meteorology Naval Postgraduate School Monterey, California 93940	1
4. Air Weather Service AWVAS/TF Scott AFB, Illinois 62225	2
5. Capt. Harry Hughes AFIT/CIPF Wright-Patterson AFB, Ohio 45433	1
6. Professor C.-P. Chang, Code 63Cp Department of Meteorology Naval Postgraduate School Monterey, California 93940	4
7. Professor K.M.W. Lau, Code 63Ly Department of Meteorology Naval Postgraduate School Monterey, California 93940	2
8. Capt. Earle L. McCormick Air Force Global Weather Central Offutt AFB, Nebraska 68113	3